ADA
0672 92

③ **LEVEL** ~~III~~   AD-E100 198

INVESTIGATION OF SPECIAL TECHNIQUES RELATED TO SATELLITE COMMUNICATIONS

FINAL REPORT

VOLUME 2 — TASK 2 "mm WAVE TECHNOLOGY"

ER78-4272 –~~AIRYA~~   25 August 1978

N+

Prepared Under

CONTRACT NO. DCA 100-77-C-0059

Prepared For

# DEFENSE COMMUNICATION AGENCY

Washington, D.C. 20305

Prepared By

RAYTHEON COMPANY
EQUIPMENT DIVISION

Communication Systems Directorate
Sudbury, Massachusetts 01776

DDC
RECEIVED
APR 4 1979
B

79 04 02 095

REPORT DOCUMENTATION PAGE		READ INSTRUCTIONS BEFORE COMPLETING FORM
1. REPORT NUMBER ER 78-4272	2. GOVT ACCESSION NO.	3. RECIPIENT'S CATALOG NUMBER
4. TITLE (and Subtitle) Investigation of Special Techniques Related to Satellite Communications-Final Report Volume 2 - Task 2 "mmWave Technology" C017037-Vol 1		5. TYPE OF REPORT & PERIOD COVERED Final
		6. PERFORMING ORG. REPORT NUMBER
7. AUTHOR(s)		8. CONTRACT OR GRANT NUMBER(s) DCA 100-77-C-0059
9. PERFORMING ORGANIZATION NAME AND ADDRESS Raytheon Company Equipment Division Communications Systems Directorate Sudbury, Mass 01776		10. PROGRAM ELEMENT, PROJECT, TASK AREA & WORK UNIT NUMBERS PE 33126K
11. CONTROLLING OFFICE NAME AND ADDRESS Defense Communications Agency MILSATCOM Systems Office (MSO) Washington, D. C. 20305		12. REPORT DATE 25 August 1978
		13. NUMBER OF PAGES 96
14. MONITORING AGENCY NAME & ADDRESS(If different from Controlling Office)		15. SECURITY CLASS. (of this report) UNCLASSIFIED
		15a. DECLASSIFICATION/DOWNGRADING SCHEDULE

16. DISTRIBUTION STATEMENT (of this Report)

Approved for public release; distribution unlimited.

17. DISTRIBUTION STATEMENT (of the abstract entered in Block 20, if different from Report)

18. SUPPLEMENTARY NOTES

Review relevance five years from submission date.

19. KEY WORDS (Continue on reverse side if necessary and identify by block number)

satellite communications
mm Wave technology
EHF
state-of-the-art

technology baseline
ground segment
space segment

20. ABSTRACT (Continue on reverse side if necessary and identify by block number)

This report described the results of developing a mm Wave Technology baseline for satellite communication systems. This baseline is applicable to a deployment frame from 10 to 15 years and covers the satellite communications bands from 20- to 100-GHz. To project the technology to such a long time span, the state-of-the-art of the mm Wave subsystems, for both the ground and space segments of satellite communication systems, were surveyed. Their limitations were investigated and, where applicable, extrapolations were made to the time frame of interest.

INVESTIGATION OF SPECIAL TECHNIQUES RELATED

TO SATELLITE COMMUNICATIONS

FINAL REPORT

VOLUME 2 — TASK 2 "mm WAVE TECHNOLOGY"

ER78-4272   25 August 1978

Prepared Under

CONTRACT NO. DCA 100-77-C-0059

Prepared For

DEFENSE COMMUNICATION AGENCY
Washington, D.C. 20305

Prepared By

RAYTHEON COMPANY
EQUIPMENT DIVISION
Communication Systems Directorate
Sudbury, Massachusetts 01776

TABLE OF CONTENTS

TABLE OF CONTENTS (Cont.)

iv

LIST OF ILLUSTRATIONS

LIST OF ILLUSTRATIONS (Cont.)

LIST OF ILLUSTRATIONS (Cont.)

vii

LIST OF TABLES

LIST OF TABLES (Cont.)

ix

FOREWORD

This Final Report presents the results of the total effort on Study Contract No. DCA 100-77-C-0059, entitled "Investigation of Special Techniques Related to Satellite Communications."

This study was performed for the Defense Communication Agency (DCA), Mr. John D. Edell, Project Manager, by Raytheon Equipment Division, Communication Systems Directorate. The Contractor's activity for Task No. 2 "mm Wave Technology" was performed by A.A. Castro and J.F. Healy.

ABSTRACT

This Final Report describes the results and conclusions on Task No. 2 of Contract DCA 100-77-C-0059, consisting of developing a mm Wave Technology baseline for satellite jam users and communication systems. This baseline is applicable to a deployment frame from 10 to 15 years and covers the satellite communications bands from 20- to 100-GHz. To project the technology to such a long time span, the state-of-the-art of the mm Wave subsystems, for both the ground and space segments of Satellite Communication systems, were surveyed. Their limitations were investigated and, where applicable, extrapolations were made to the time frame of interest.

SECTION 1

INTRODUCTION

The objective of this study task is to investigate and extrapolate the millimeter wave technology base for satellite communication systems that may be deployed in a 10 to 15 years time frame. This technology base comprises both communication systems and ECM threats (jammers) and includes the following bands currently assigned to satellite communications:

20/30 GHz	K band
40 to 45 GHz	Q band
50 to 51 GHz	U band
59 to 64 GHz	U & V band
66 to 71 GHz	V band
92 to 95 GHz	W band
95 to 101 GHz	W band

The most current military oriented space communication technology (both space and ground segments) at mm wave frequencies, have been developed during the Lincoln Experimental Satellite (LES) 8 and 9 experiment, for the up, down and cross-links at upper K_a-band. Other operational equipment at mm wave frequencies was developed for the ATS-6 propagation experiments, the Japanese CS satellite and for radio astronomy applications.

It is apparent that although there are many systems on the planning boards, limited amount of experience has been accumulated on actual hardware for satellite mm wave communication systems. In order to project a technology baseline to a long span of time such as 10 to 15 years, it is required not only to survey the current "state-of-the-art" of subsystems and components, but to look into the physics of the devices and their limitations.

The subsystems and components to be used as building blocks for a mm Wave satellite communication system are summarized in Table I, which also indicates the

1-1

Table I. mm Wave (20-100 GHz) Satellite Communication Technology Summary

	TYPE	TYPICAL APPLICATION
FREQUENCY SOURCES	GUNN DIODE	UP DOWNCONVERTERS LO PARAMETRIC AMPLIFIER PUMPS
	IMPATT DIODE	LIMITED BY NOISE CHARACTERISTICS
	MULTIPLIERS	UP DOWNCONVERTERS LO PARAMETRIC AMPLIFIER PUMPS
	FREQUENCY SYNTHESIZERS	FREQUENCY HOPPING
SOLID STATE AMPLIFIERS	TDA	LOW NOISE AMPLIFIER
	GUNN DIODE	DRIVERS
	IMPATT DIODE	SPACE POWER AMPLIFIERS
	FET	LOW NOISE AMPLIFIERS DRIVERS LIMITED IN FREQUENCY COVERAGE
	PARAMETRIC AMPLIFIERS	LOW NOISE AMPLIFIERS
	MASER	LIMITED APPLICATION
DOWNCONVERTERS	SCHOTTKY BARRIER	
	SUPER SCHOTTKY	VERY LOW NOISE FIGURE LIMITED APPLICATION
	HARMONIC MIXERS	LOWER LO FREQUENCY HIGHER NOISE FIGURE
	PARAMETRIC DOWNCONVERTER	SPACE APPLICATION
	JOSEPHSON JUNCTION	EXTREMELY LOW NOISE FIGURE LIMITED APPLICATION
	FET MIXER	LIMITED FREQUENCY COVERAGE
UPCONVERTERS	PARAMETRIC, RESISTIVE	
MODULATORS	VARIABLE PATH LENGTH	DIRECT HIGH SPEED DIGITAL MODULATION
TWT	HELIX	POWER LIMITED, SPACE APPLICATION
	COUPLED CAVITY	GROUND TERMINAL AND SPACE APPLICATION
KLYSTRONS	REFLEX	PARAMETRIC AMPLIFIER PUMPS, BECOMING OBSOLETE
	AMPLIFIER	VERY LIMITED APPLICATION
MAGNETRON		VERY LIMITED APPLICATION
GYROTRONS		EXTREMELY HIGH POWER LIMITED APPLICATION
RELATIVISTIC BEAMS		EXTREMELY HIGH POWER VERY LIMITED APPLICATION
TRANSMISSION MEDIA	COAXIAL	LIMITED IN FREQUENCY COVERAGE
	RECTANGULAR WAVEGUIDE	
	CIRCULAR WAVEGUIDE	LOWEST LOSSES LIMITED APPLICATION
	MIC TECHNIQUES	HIGHER LOSSES LIMITED APPLICATION
ANTENNAS	REFLECTOR TYPE	GROUND AND SPACE
	LENS	GROUND AND SPACE LIMITED APPLICATION
	PHASE ARRAY	GROUND LIMITED APPLICATION
RADOMES	INFLATABLE	
	METAL FRAME	
	THICK RADOMES	LIMITED APPLICATION

technology used at these frequencies and the typical application and limitations. In the following paragraphs, a summary overview is given on the state of the art of the realization of these mm wave devices, components and subsystems and their extrapolation to the time frame of interest.

SECTION 2

SOLID STATE DEVICES

In the development of mm wave satellite communications systems, the same generic devices that may be found at lower microwave frequencies, i.e., oscillators, amplifiers, frequency converters, modulators and detectors, are still used. This section will give the status of each of these solid state devices via a performance breakdown of the major components in that device classification, and extrapolate their characteristics into the time frame of interest.

2.1 FREQUENCY SOURCES

The frequency sources, that will find major use in millimeter-wave systems, will have the form of the following:

- fundamental oscillators, using GUNN or IMPATT type diodes
- low frequency oscillators followed by harmonic multipliers
- frequency synthesizers

2.1.1 GUNN DIODE OSCILLATORS

GUNN diodes, operating as stable microwave frequency sources, have been available for the last ten years. Over that period the frequency range has been extended from X-band to over 100 GHz and the CW power level increased to produce as much as 30 mW at 94 GHz.

The primary GUNN oscillator work has been done with n-type Gallium Arsenide (GaAs) with the doping configuration of Figure 2-1. The oscillator circuits that have been used have the diode mounted in the narrowband waveguide structure of Figure 2-2 or the broadband coax-waveguide structure of Figure 2-3. A common circuit technique used in the highest power oscillators below 50 GHz has two GaAs diodes mounted inseries in the coaxial structure. The current and projected output power and tuning range of the GUNN oscillator is given in Figure 2-4.

2-1
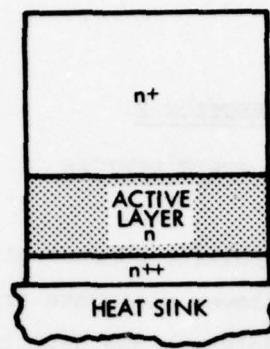
Figure 2-1. GUNN Diode Doping Configuration
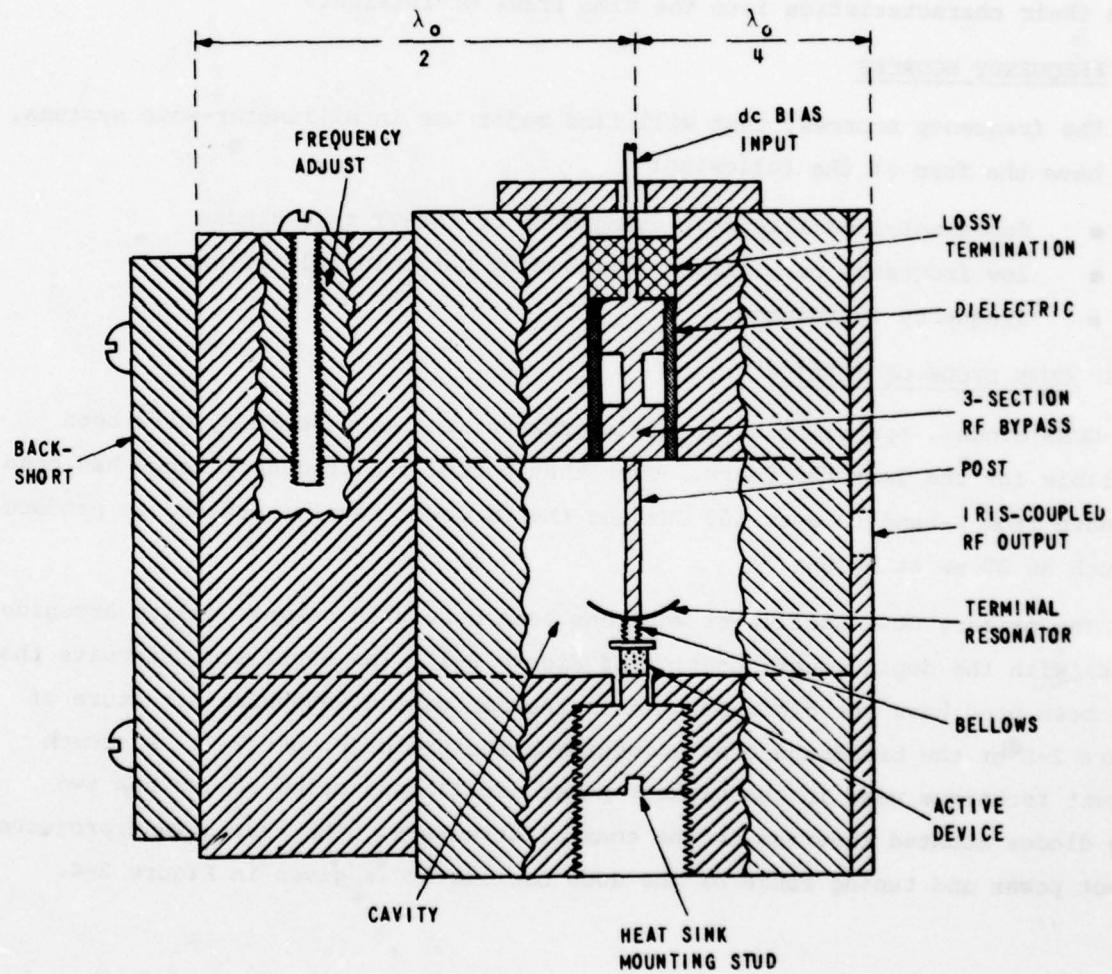
Figure 2-2. Narrowband Waveguide Oscillator Circuit

DC BIAS

GUNN
DIODE
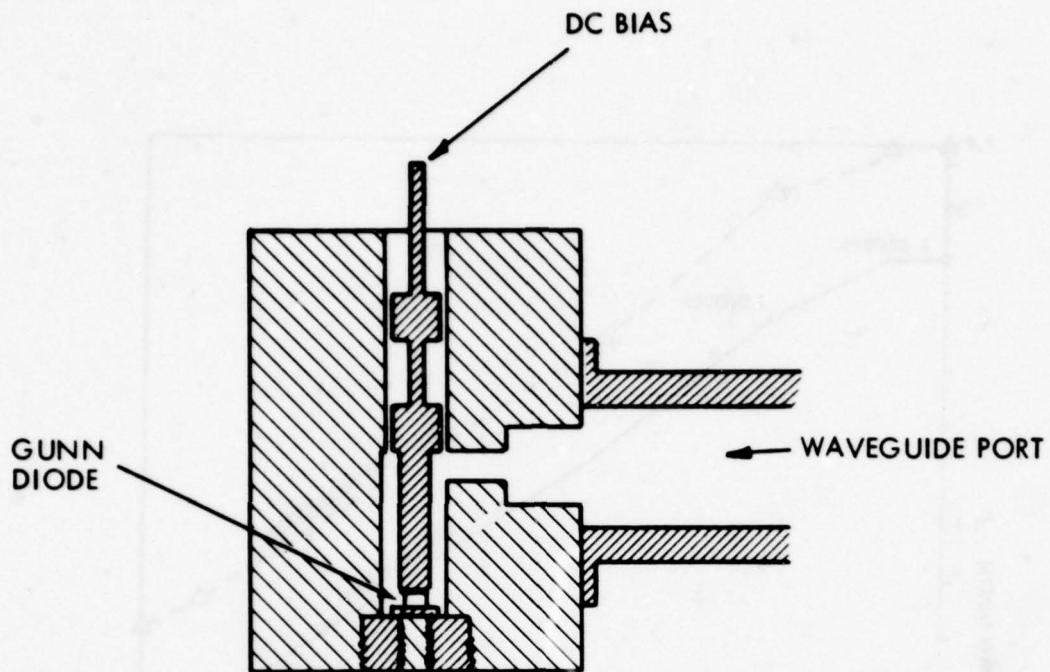
WAVEGUIDE PORT

Figure 2-3. Broadband Coax-Waveguide Oscillator Circuit

The most significant improvement in GUNN diode power will be the use of Indium Phosphide (InP). The InP material has an electron velocity characteristic that is double that of GaAs. From the general power-frequency equation for GUNN devices

$$P_o f^2 \sim K, \text{ where K is a constant proportional to the electron velocity.}$$

the expected increase in the GUNN diode oscillator power will be 3 dB.

Although the GUNN diodes are relatively new devices, sufficient reliability information has been obtained to consider them for space systems. For instance, Central Microwave Corporation has already developed a 55 GHz oscillator for a satellite application.
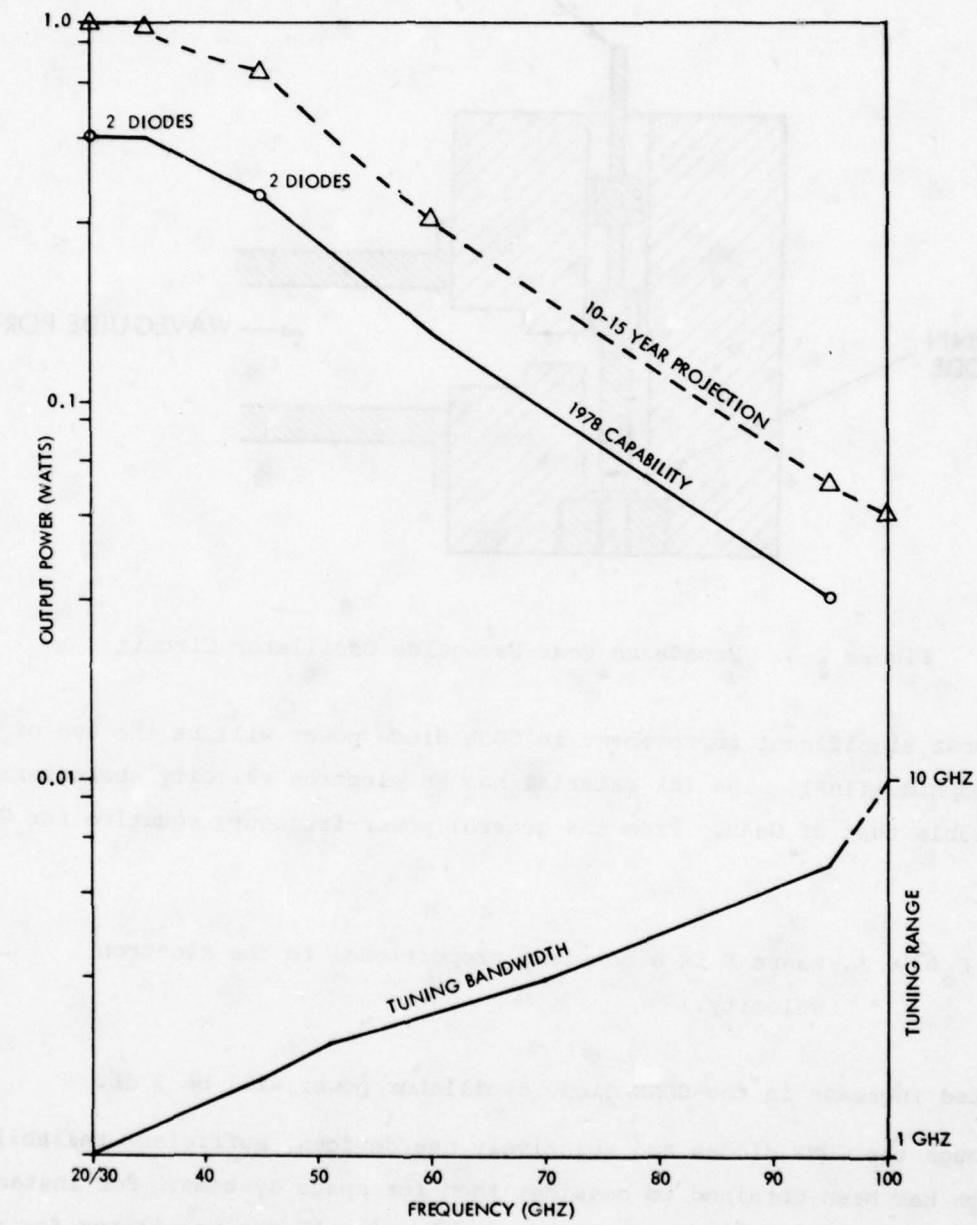
Figure 2-4. GUNN Diode Oscillator Performance

2.1.2 IMPATT DIODE OSCILLATORS

The IMPATT diode oscillator has been available a few years longer than the GUNN device and has experienced the same steady improvement in power and frequency. The power obtainable from the IMPATT device is greater than available from the GUNN diodes of Section 2.1.1 but at the expense of higher noise and higher operating voltages.

The IMPATT diode device is a simple p-n junction as shown in Figure 2-5 that is reversed biased into a negative resistance region. The negative resistance results from a combination of internal secondary emission (or avalanche) and carriers moving at saturation drift velocities. The optimization of the microwave circuit and bias current produces a microwave oscillator that can produce up to a 1 watt CW at 60 GHz.[*] The current and projected output power and tuning range of oscillators using silicon diodes is given in Figure 2-6. Most of the improvement in IMPATTS, to obtain the current power levels, has been made recently with the development of the double-drift Silicon diode with diamond heat sink package. This diode provides a more efficient removal of the heat dissipated in the active portion of the device.
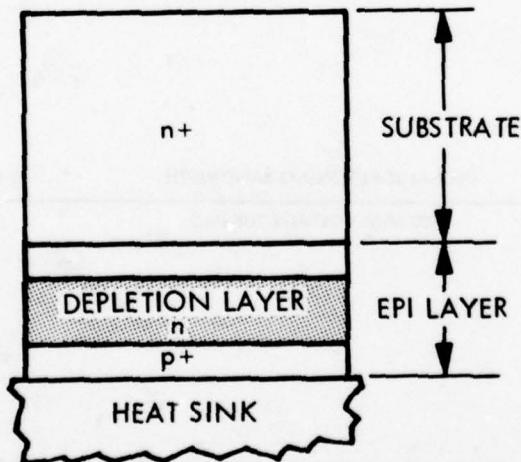
Figure 2-5.   IMPATT Diode Device

---

[*] H.J. Kuno and T.T. Tomg, "Solid-State Millimeter-Wave Sources", IEEE EASCOM-77 Proc, 24-2, Sept. 1977.
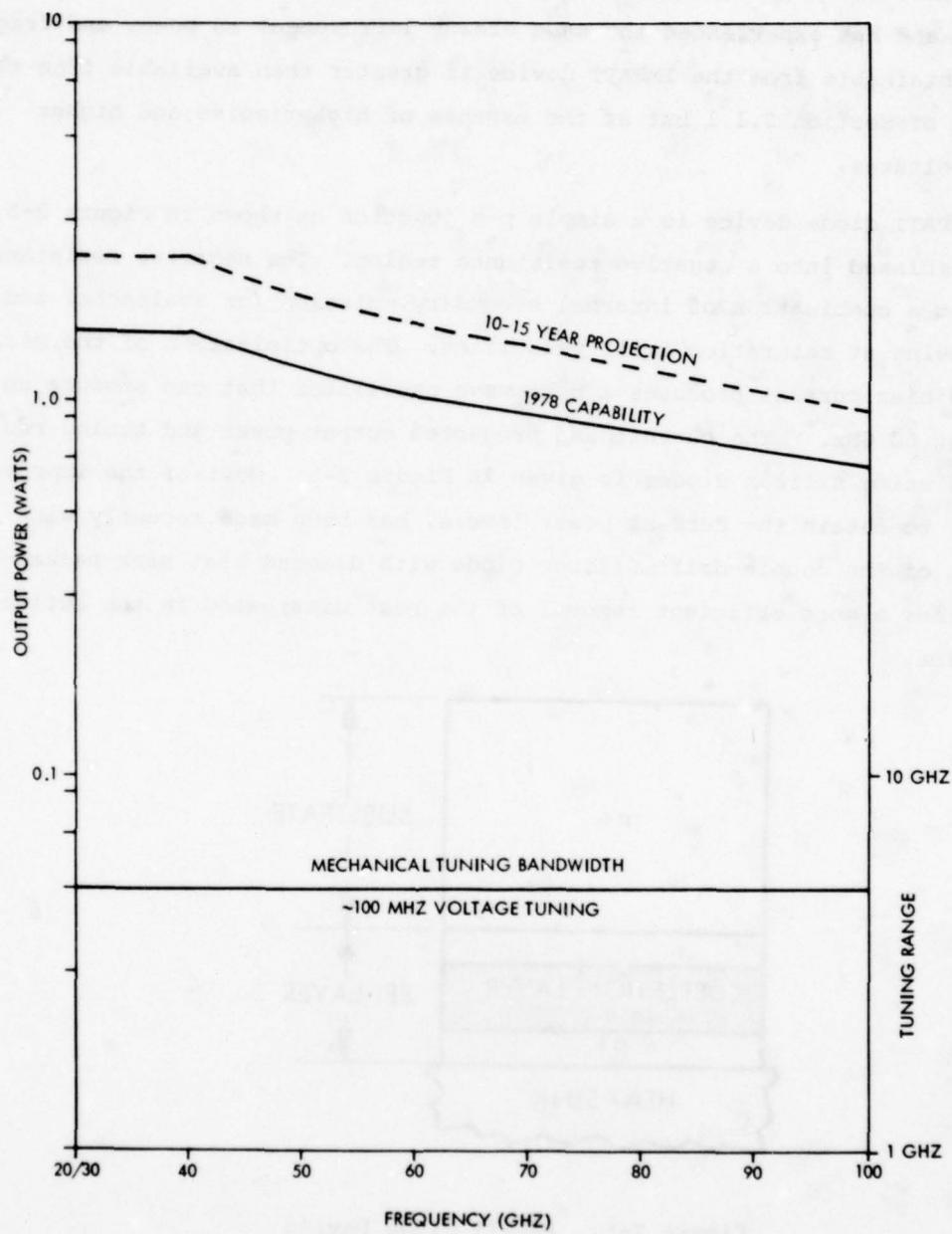
Figure 2-6.   IMPATT Diode Oscillator Performance

The heat removal from the diode has been the limiting factor in the IMPATT reliability performance. In order to get an expected operating life of greater than 10,000 hours the IMPATT manufacturers have had to put a limit of 250°C on the maximum junction temperature.

Like the GUNN diode the most significant improvement in the IMPATT diode power will be from a change in material. The development of the Gallium Arsenide (GaAs) diode, with its higher mobility and lower series resistance, will bring a typical 2 dB improvement over the current RF output power. Additional improvement in the circuit design is expected which will have active tuning elements, such as varactors, integrated with the diodes to achieve broad voltage tuning ranges. Presently the devices have a 5 GHz mechanical and 100 MHz voltage tuning range.

The long term development will not see much of an improvement in noise performance of the IMPATT device. Because it operates on an avalanche process the device has a higher inherent noise (both AM and FM) characteristic than GUNN devices. The current noise degradation of the IMPATT is typically 10 to 15 dB higher than the GUNN. The use of the GaAs diode is expected to bring the degradation to 10 dB which still precludes their use in receiver front ends but does not inhibit high power applications.

For space applications IMPATT devices at 38 GHz have been used aboard the LES 8/9 satellite system. These devices have proved reliable over the present life of that millimeter-wave system.

2.1.3 MULTIPLIERS

With the increasing availability of GUNN diode oscillator producing better than 30 mW up to 94 GHz the interest in high power frequency multipliers over the 20 to 100 GHz has diminished sharply. The main emphasis in multiplier work has changed to frequency bands well above 100 GHz, where GUNN and IMPATT devices have not been started, and to low power, broad-band sources for phase-lock applications under 100 GHz.

The present work in frequency multipliers has been with Silicon (Si) and Gallium Arsenide (GaAs) varactors to achieve efficient multiplier stages. Emphasis has been placed on low multiplication stages, X2 and X3, and their associated cascaded chains. Presently the single diode doubler stages with input

of 0.5 watt at 15 GHz produce conversion efficiences of 35%. Tripler stages
with inputs at 30 GHz have conversion efficiences of almost 30%. Cascaded chains
of the two stages have an overall conversion efficiency of 10%, producing 50 mw
over a 1 GHz bandwidth at 94 GHz.

Present development effort is being spent on variations of the X2 and X3
multiplier stages to cover the whole frequency band to 100 GHz and to improve the
overall bandwidth. The existing multipliers are waveguide mounted diodes with
cavities on the resonant elements. The largest bandwidth expected from this
approach is about 3 GHz for the 10% conversion efficiency.

Long term development is still planned in the low power multiplier stages with
the emphasis being placed in increasing bandwidth and the introduction of integrated
circuits with beam-lead type diodes in a microstrip type package. The expected
bandwidth of these new devices is typically 5 GHz with 10% conversion efficiency.

Frequency multipliers using varactor diodes are not new to space systems.
Many variations have been built and flown aboard satellite systems so limitations
do not exist for these devices discussed.

2.1.4 SYNTHESIZERS

The large bandwidth available at mm wave satellite communication bands are
ideally suited for spread spectrum AJ modulation, in particular frequency hopping.
Hopping synthesizers at mm wave capable of ground and space operation have been
developed. The main characteristics which define the performance of a frequency
hopping synthesizer are:

- Resolution
- Settling time
- Spectral purity
- Hopping bandwidth
- Power consumption volume and weight for space applications

In order to obtain high resolution the frequency steps must be generated at
sufficiently low frequency and all frequencies used in the generation scheme must
be locked to a common high stability standard. The settling time determines the
highest hopping rate that may be achievable and it depends on the synthesis method.

Spectral purity will be one limiting factor for low data rate and extremely large AJ gain, communications at mm Wave frequencies[*]. The required hopping bandwidth also determines the method of frequency synthesis to be used. Power consumption, volume and weight may be minimized by the choice of components and construction techniques.

The state of the art of a hopping synthesizer design for mm Wave satellite communications will be illustrated by a hopping synthesizer capable of covering the 36 to 38 GHz, and where direct synthesis is used to achieve a settling time of less than 1.5 μsec, edge to edge of the 2 GHz bandwidth. In the block diagram of Figure 2-7, the fine hopping synthesizer is a mix and divide type, which is inherently modular allowing all stages to be identical and share a common set of comb frequencies with a fixed separation. In the space version, this synthesizer is built with thick film integrated circuitry modules, having two substrates which contain a 4PST switch, frequency selection circuitry, mixer, divide by four circuit and amplifier. Six of these modules, each having 250 mW dissipation, were assembled into a synthesizer as shown in Figure 2-8 for the ground and space (hybrid IC) versions.

---

[*] A.A. Castro, F. Ziolkowski "Generation of mm Wave signals of high spectral purity" MTT Transactions, Special Issue on mm Waves, Nov. 1976.

70 MHZ
IF
INPUT SIGNAL

36650-38598
OUTPUT SIGNAL

U C   1030 MHZ   D C   698±128   D C   3270-2256   U C   34304 OR 35328

960

1728 ±.08N   X32   52±.0025N

34304 OR 35328   X4

8832   SPDT   8576

FINE HOPPING

N 0 TO 1600

3840   3584   3328   3072   SP4T

12 bits

2 bits

1 bit

FIXED FREQUENCY GENERATOR

STD
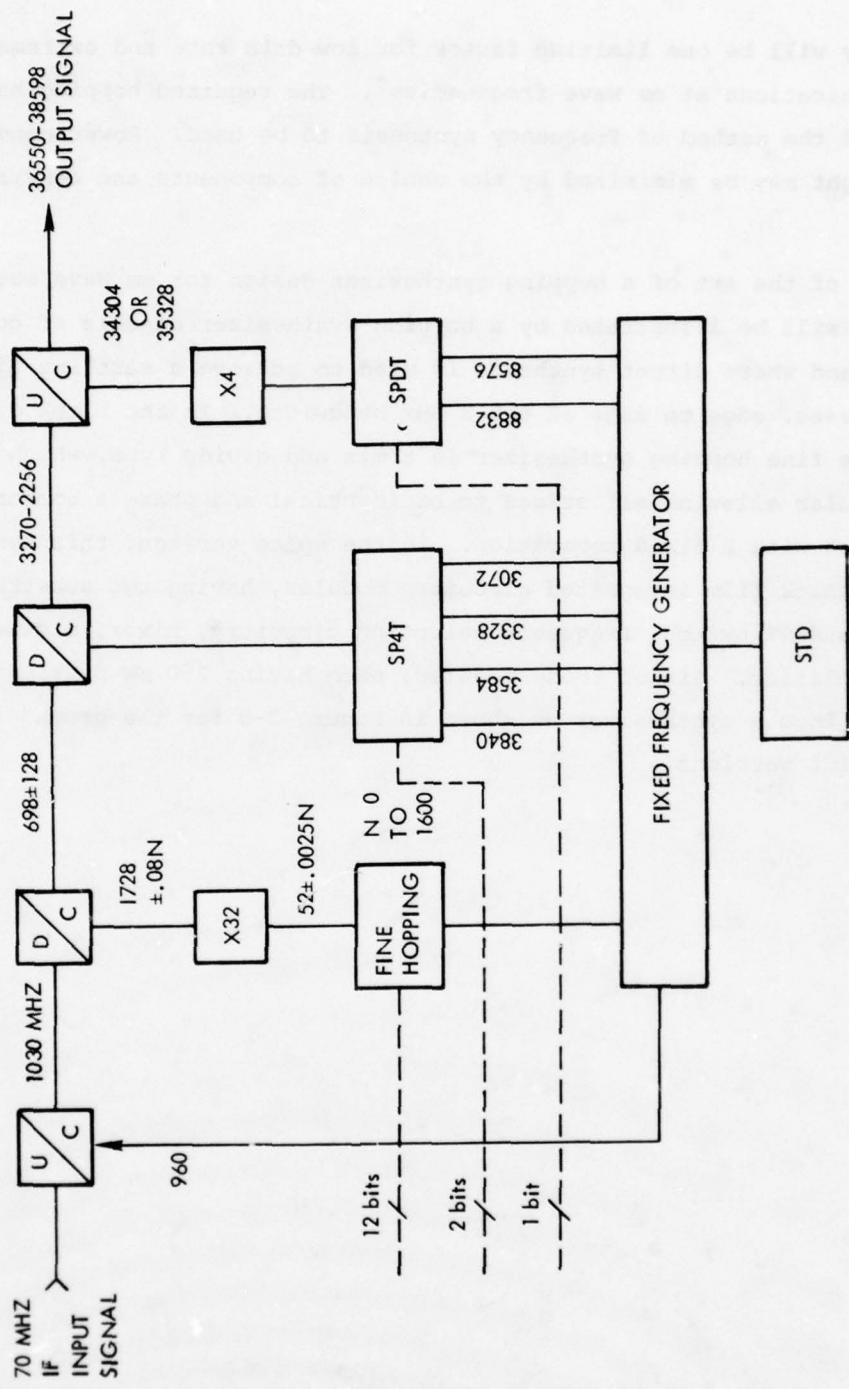
Figure 2-7. Hopping Synthesizer (Transmit)
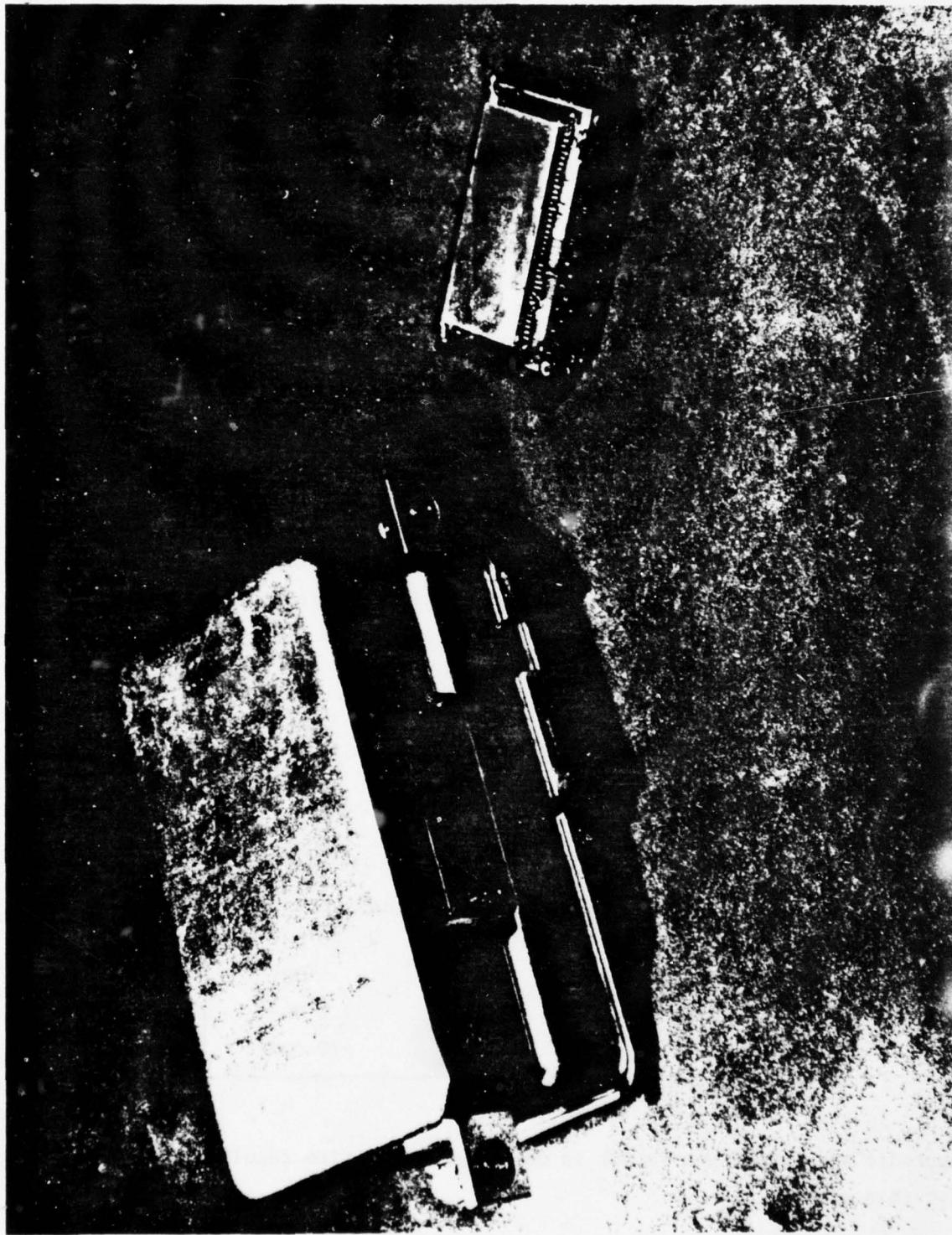
Figure 2-8. Fine Hopping Synthesizer Ground and Space Versions

2.2 AMPLIFIERS

A variety of solid state amplifiers exist in the frequency range of this study. They include the following:

- FET
- GUNN Diode
- IMPATT Diode
- Parametric
- Tunnel Diode

These amplifiers have a wide range from low noise, low power to high noise, medium power with very little overlap of usage. In this section each will be addressed for its current status and projected capability.

2.2.1 FET AMPLIFIER

With the introduction of the GaAs Field Effect Transistor (FET) in the last five years the device has just about taken over the amplifier market in the frequency range from 2 to 18 GHz. The ease at which device capability has been achieved up to 18 GHz has stimulated some manufacturers to extend their interest beyond the major market areas.

Some work has been done on the GaAs FET at 20 GHz with 0.5 micron wide gate. Typical characteristics are given in Table II.

Table II. Current FET Work at 20 GHz

Frequency	20 GHz
Single Stage Gain	6 dB
Noise Figure	7.0 dB
Power Output	+10 dBm

Sporadic work at 26 and 30 GHz is going on but no firm results were available for this study.

Long term projection shows some plans to reach 40 GHz with considerable device development and circuit improvements. Balanced amplifier stages are expected to be necessary in order to achieve a reasonable power level of +10 dBm.

For satellite applications, C-band GaAs FET amplifiers have already been space qualified. Considering the long term development projection and the required space qualification program the GaAs FET amplifier should only be considered for satellite systems under 30 GHz.

2.2.2 GUNN DIODE AMPLIFIERS

The GUNN diode amplifier is basically an oscillator module, described in Section 2.1.1, assembled with ferrite circulators in the reflection type configuration of Figure 2-9. The stages are broadband matched to achieve stable amplification over wide bandwidths. The current and projected performance of the GUNN amplifier is given in Figure 2-10. The output power of the amplifier is typically 1 to 2 dB below that obtained from oscillators. This results from
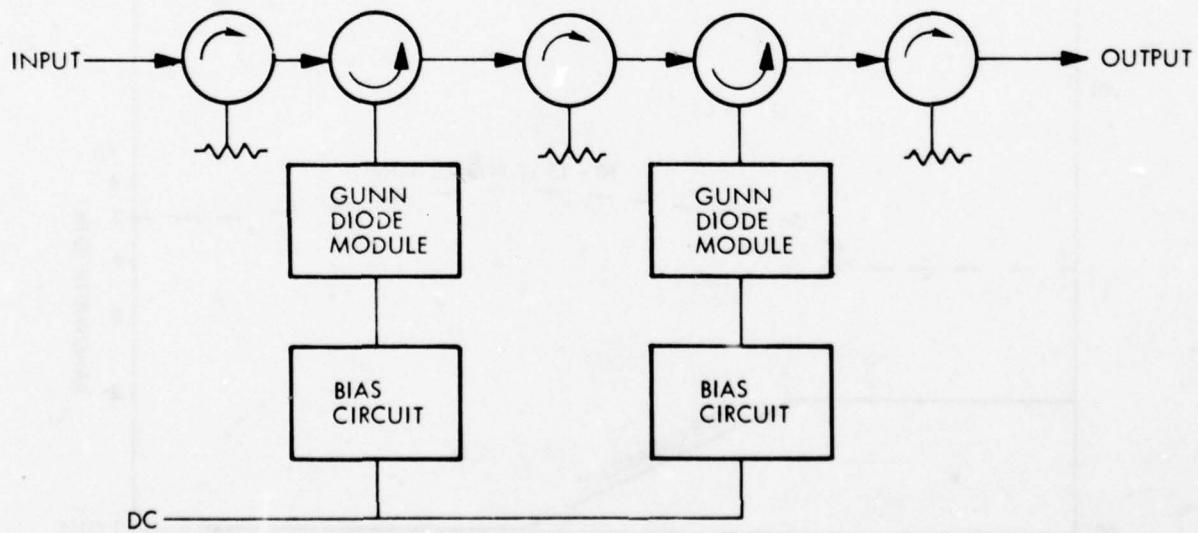
Figure 2-9. GUNN Diode Amplifier Block Diagram

2-13
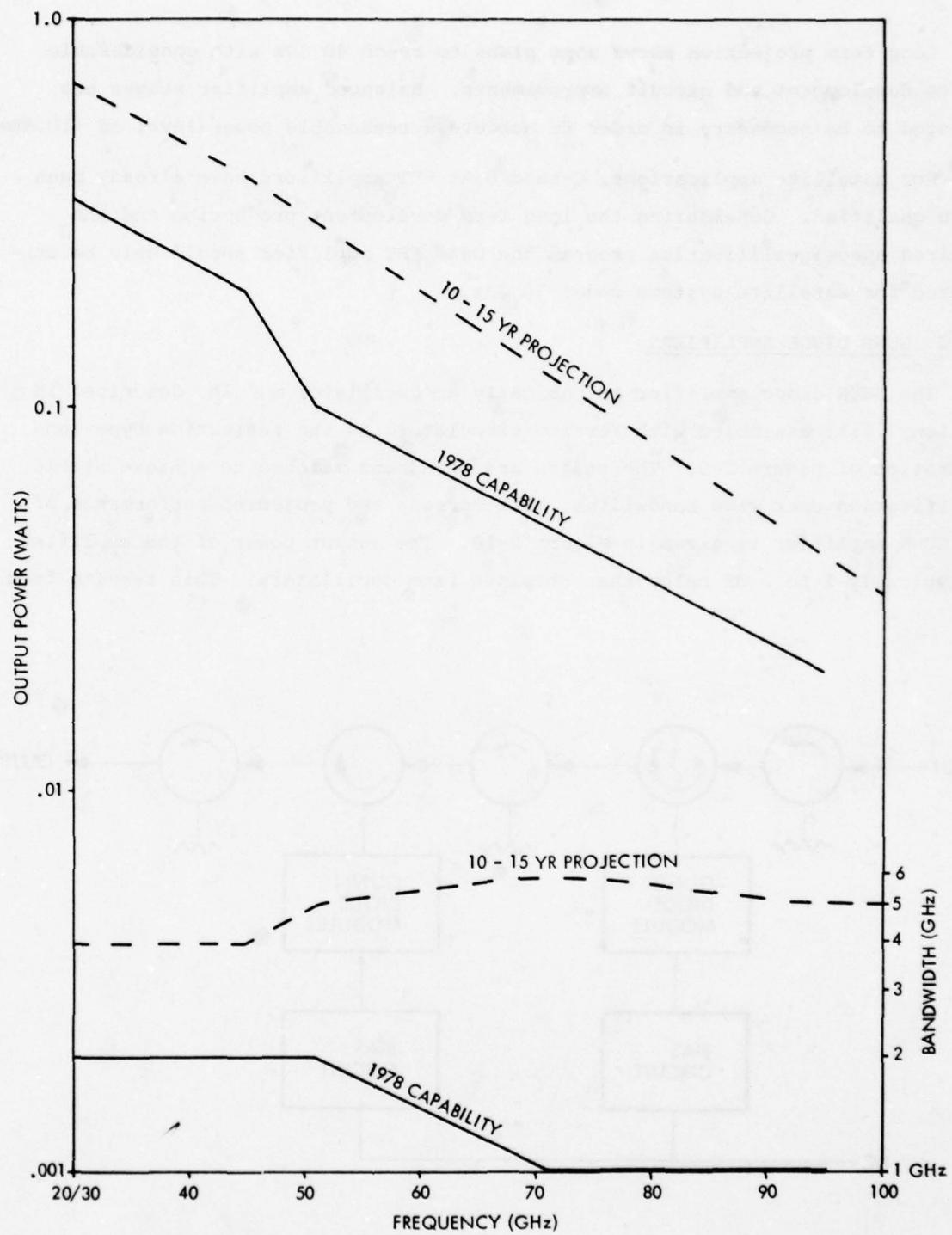
Figure 2-10. GUNN Diode Amplifier Performance (No Power Combining)

the low Q circuits and the insertion loss of the ferrite devices. The Noise
Figure of the GUNN diode amplifier does not show a dramatic change from 20 to
100 GHz. The typical Noise Figure at 20 GHz is about 18 dB and at 100 GHz is
about 22 dB.

Presently higher output power can be achieved with hybrid combining tech-
niques as shown in Figure 2-11. A 4-way combiner is capable of increasing output
power by 5 dB over the single amplifier device, with only about 10% loss in
bandwidth.

Another technique to achieve higher power is the injection locked oscillator
configuration of Figure 2-12. This technique achieves the output power of the
oscillator with an input signal level of 15 to 20 dB below the output level but
does it with considerable reduction in bandwidth. Devices have been built that
operate with input signals at the fundamental as well as its subharmonics.
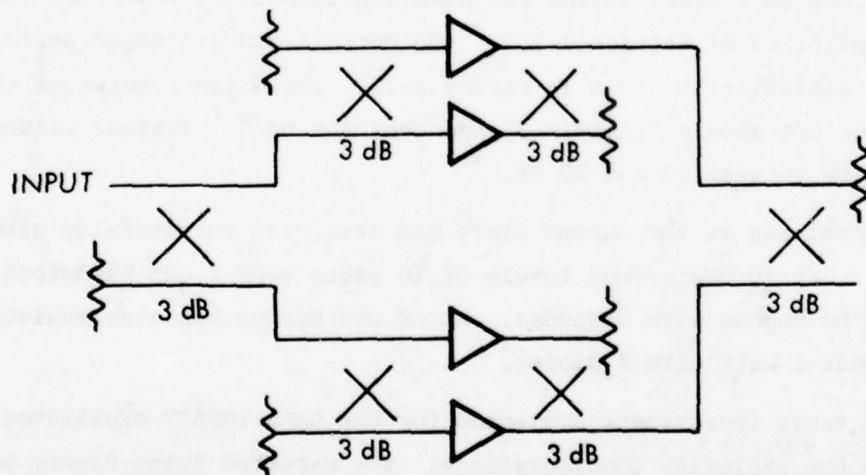
Figure 2-11. 4-Way Amplifier Combiner Technique

INPUT ─────── (⟳) ─────── OUTPUT

GUNN
DIODE
OSCILLATOR
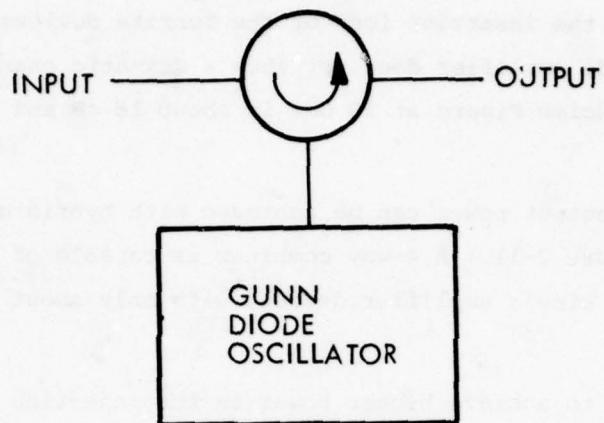
Figure 2-12. Injection Worked Oscillator Technique

The major improvement for the GUNN diode amplifier will be the development
of the Indium Phosphide (InP) diode. As described for the oscillator a 3 dB
improvement in putput power will be realized. An improvement of almost 4 dB in
noise figure will also be achieved in the amplifier devices.

2.2.3 IMPATT DIODE AMPLIFIER

IMPATT diode amplifiers follow the same configurations described for the
GUNN diode amplifiers of Section 2.2.2. The current and projected performance
of the IMPATT amplifier is given in Figure 2-13. The Noise Figures of the
IMPATTS also do not show a dramatic change over the band. Typical values of
Noise Figure are between 33 and 35 dB.

Hybrid combining at the output stage has been used successfully with the
IMPATT diodes. At 30 GHz output levels of 10 watts over 1 GHz bandwidth have
been achieved by Hughes with 8 diodes. At 60 GHz Hughes has also achieved
levels of almost 1 watt with 4 diodes.

The long range improvement projected for the GaAs IMPATT oscillator will be
applicable to the amplifier configurations. The expected Noise Figure of the
IMPATT amplifiers will be near 30 dB.
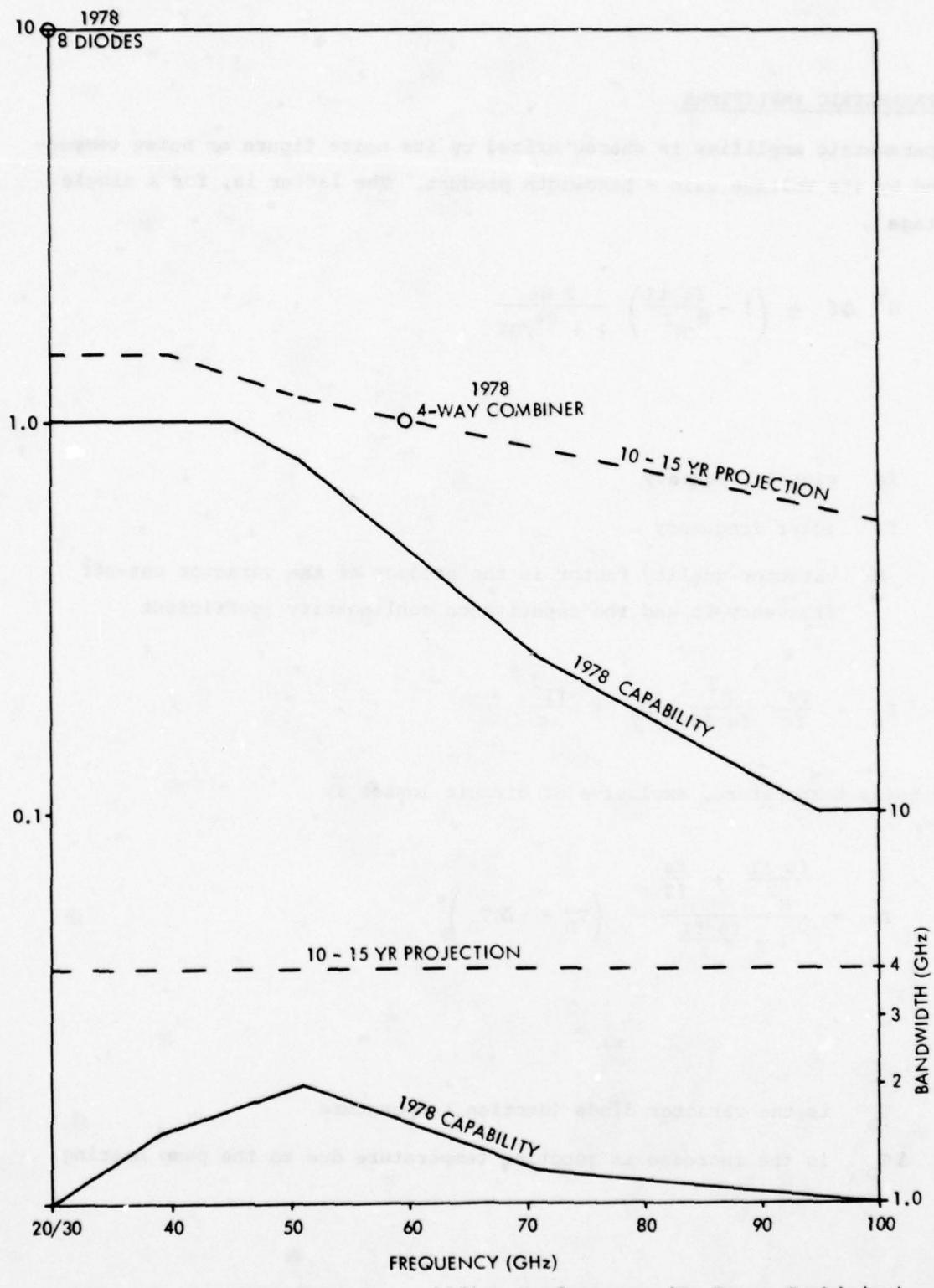
Figure 2-13. IMPATT Diode Amplifier Performance (No Power Combining)

2.2.4 PARAMETRIC AMPLIFIERS

A parametric amplifier is characterized by its noise figure or noise temperature and by its voltage gain - bandwidth product. The latter is, for a single tuned stage

$$G^{\frac{1}{2}} \, \Delta f \;=\; \left(1 - \frac{fs \; fI}{M^2}\right) \frac{2 \, Bs}{1 + Bs/BI}$$

where

    fs   signal frequency

    fI   idler frequency

    M   varactor quality factor is the product of the varactor cut-off
         frequency fc and the capacitance nonlinearity coefficient

and

$$B_S \;=\; \frac{fs^2}{fc} \; \frac{M^2}{fs \; fI} \;,\; B_I \;=\; \frac{fI^2}{fc}$$

and the noise temperature, exclusive of circuit losses is

$$Te \;=\; \frac{\dfrac{fs \; fI}{M^2} + \dfrac{fs}{fI}}{1 - \dfrac{fs \; fI}{M^2}} \left(T_D + \Delta T_D\right)$$

where

    T_D is the varactor diode junction temperature

    ΔT_D is the increase in junction temperature due to the pump heating

2-18

The paramp noise temperature is then determined by the pump frequency (fp = fs + fI), the varactor figure of merit and junction temperature. Low noise temperatures may be achieved by high pump frequency, large varactor figure of merit and cryogenially cooling the diode junction.

At mm wave frequencies there are limitations on how high the pump frequency can be with respect to the signal frequency and on the achievable varactor cut off frequency. In addition, there are practical effects which will cause the performance to be significantly poorer than that anticipated by the above theoretical estimates. These deviations are caused by the reactances associated with varactors and mounts, and RF mode conversion. Although the stray reactances do not influence the noise temperature, it is affected by the varactor and mount dissipative losses. A summary of the characteristics of uncooled (thermo-electrically stabilized) and cryogenically cooled parametric amplifiers built at the bands of interest is given in Table III.

Table III. mm Wave Parametric Amplifiers

FREQUENCY	COOLING	NOISE TEMPERATURE/ NOISE FIGURE	BANDWIDTH MHZ	MANUFAC-TURER
19 GHZ	C	115°K	600	
19 GHZ	C	60°K	2500	NEC
19 GHZ	U	3.5 DB	2500	NEC
20 GHZ	U	3.3 DB	300	SCI
20 GHZ	U	3 DB	1000	COMTECH
22 GHZ	C	100°K	1000	AIL
30 GHZ	U	4.8	300	SCI
36-38 GHZ	U	3.8	100	AIL LNR
70 GHZ	U	6.3	670	AIL
94 GHZ	U	1000°K	2000	AIL

As an example, one of the 36-38 GHz uncooled paramp developed for the LES 8/9 ground terminals given in Table III, consist of two independent paramps, each a single stage, nondegenerative, tuned to its assigned frequency, having a configuration shown in Figure 2-14 and the characteristics of Table IV.
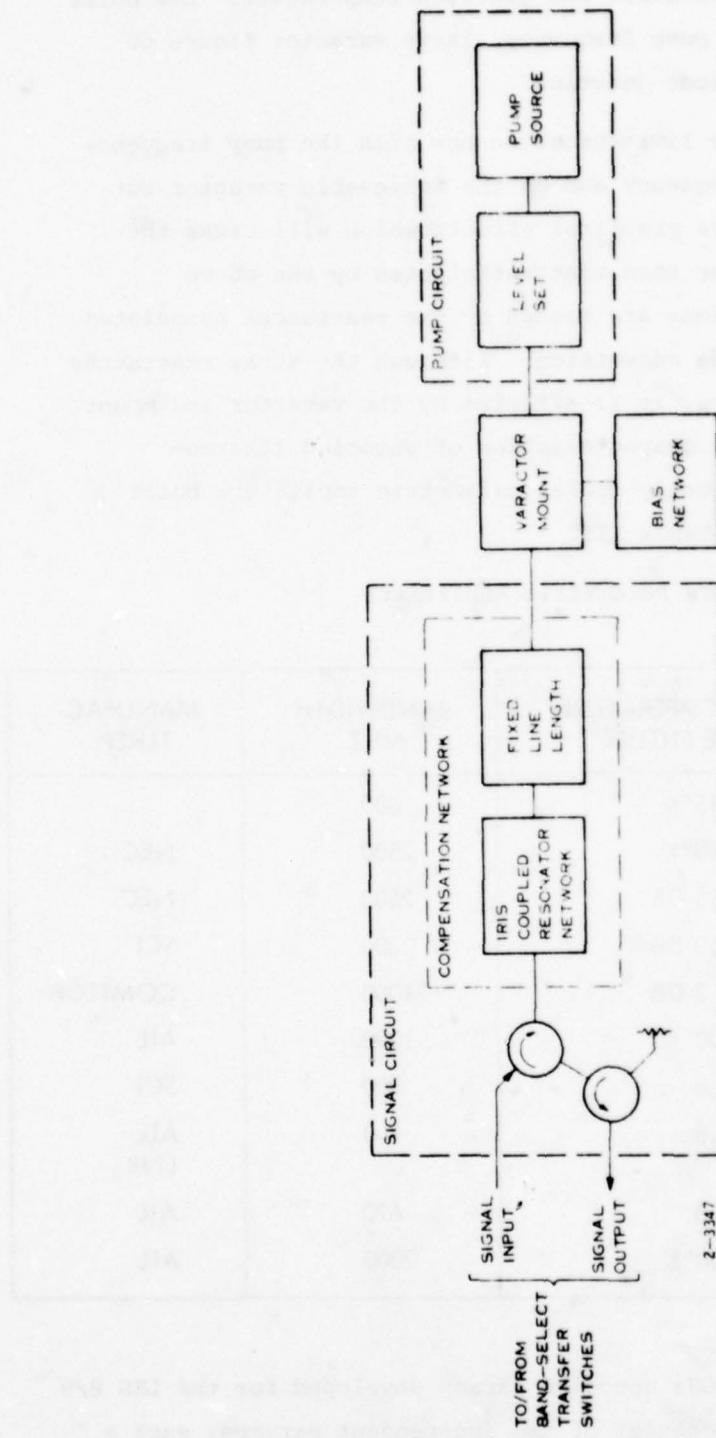
Figure 2-14. LES 8/9 Parametric Amplifier Configuration

Table IV.   LES 8/9 Parametric Amplifier Characteristics

Frequency, Band 1	36.87 ±0.05 GHz
	38.01 ±0.05 GHz
Gain	18 dB minimum
Gain Stability	±0.5 dB/24 hours, minimum
Noise Temperature	500°K
Noise Figure (LNA)	4.5 dB
Input VSWR	1.3 maximum
Dynamic Range	1 dB gain compression at an input level of -15 dBm
Pump Frequency	101.4 GHz
Pump Power	20 mW

The pump circuit operates at 101.4 GHz which is obtained by frequency doubling of the output of a 50.7 GHz Gunn oscillator. Electromechanical tuning (band selection) is accomplished with remotely controlled solenoid-driven transfer switches.

Figure 2-15 shows the paramp circuit. The varactor diode is operated near series resonance at the idler frequency. An idler cavity is created by the pump resonant iris effectively placing a low impedance a half guide wavelength from the plane of the diode at the idler frequency. The idler is isolated from the signal circuit with an iris resonant at the signal frequency. Signal circuit resonance is achieved by adjusting the ridge waveguide length from the varactor to the large discontinuity between the ridge and WR-22 waveguides. The signal circuit is isolated from the pump circuitry by a resonant iris located a quarter wavelength from the plane of the varactor at the signal frequency. The amplifiers
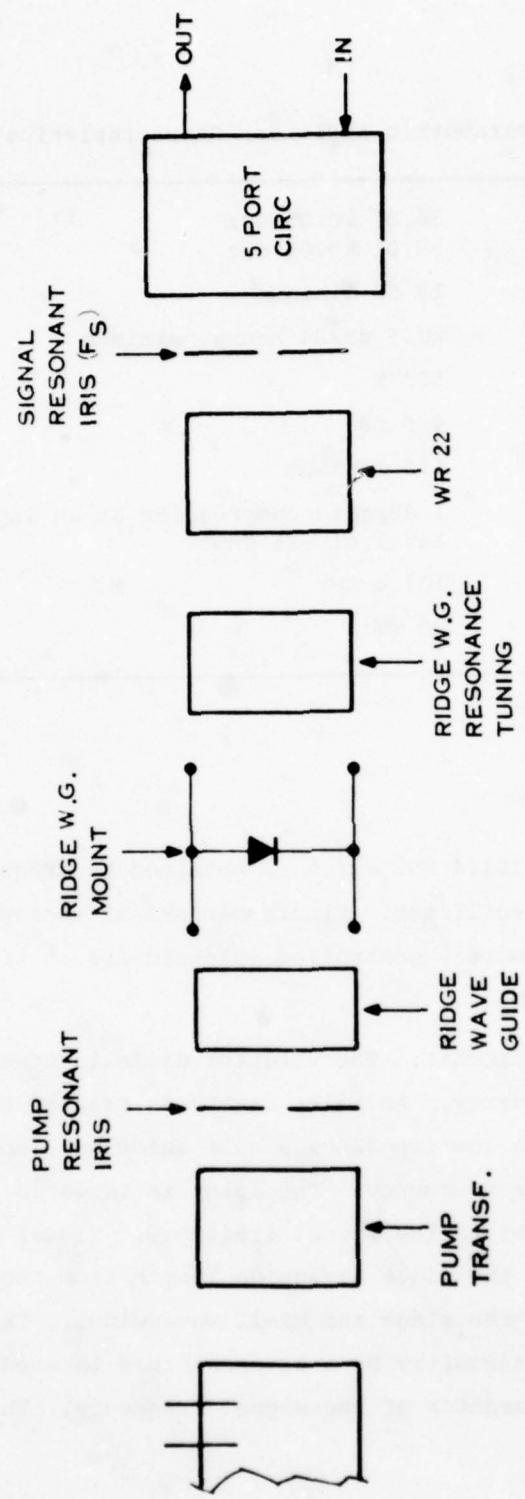
Figure 2-15. LES 8/9 Parametric Amplifier Circuit

are positioned on a plate which is thermally stabilized at 77 $+2^{\circ}$F by a proportionally controlled Peltier heating/cooling module. Heat is transferred away from the Peltier module by circulating coolant through the "cold junction" of the module. This module will either heat or cool the paramps, relative to the system heat sink depending on the polarity of the dc bias applied to the module. The temperature of the module is controlled by controlling the dc power to the module.

In addition to its use in ground stations, paramps may be incorporated in spacecraft transponder receivers. This tendency was successfully (1000 hrs space operation) started with the Canadian CTS 14 GHz paramp, and may be attractive for mm wave uplink or crosslinks. For this application, not only nondegenerate paramps are of interest but also degenerate parametric downconverters. The later result in lower pump frequency, given by

$$fp = \frac{fin + fout}{2} \, ,$$

and the idler frequency is at the difference between input (fin) and output (fout) frequencies. Figure 2-16 shows a 30 GHz space parameter downconverter (30 to 20 GHz) developed for ESA, having a 10 dB gain, 300 MHz bandwidth and a noise figure of 6 dB.

2.2.5 <u>TUNNEL DIODE AMPLIFIERS</u>

For the frequency plans used in this study the Tunnel Diode Amplifier (TDA) has only limited application. TDA's have been built in the region of 20 to 26 GHz, however, the noise and bandwidth performance is comparable to a down converter using a mixer-amplifier. The current performance of the low frequency TDA is given in Table V.

Projected performance, at higher frequencies and in time, shows no basic limitations, however, major improvements are not significant to select the TDA over an improved mixer-preamplifier.

2-23
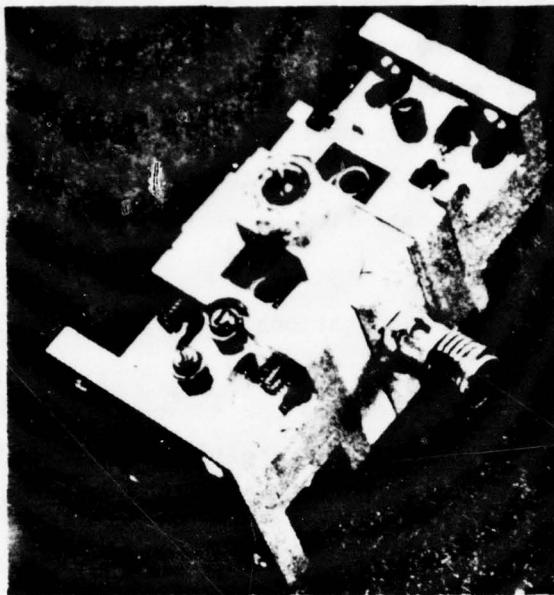
Figure 2-16.   30/20 GHz Parametric Downconverter

Table V.   Current Tunnel Diode Performance

Frequency	26 GHz
Bandwidth	2 GHz
Noise Figure	7.5 dB
Gain per stage	10 dB
Power Out (1 dB Gain Compression Point)	-20 dBm
Diode Type	Micro-pill Germanium

2.3 DOWN CONVERTERS

A variety of mixer-IF preamplifiers exist across the frequency range of this study and have noise figure characteristics comparable to X-band systems developed 10 years ago. Table VI gives the current and projected characteristics of these devices. These units are balanced mixers using Silicon Schottky barrier diodes

Table VI. Down Converter Characteristics

LEGEND: CURRENT (PROJECTED)

FREQUENCY (GHZ)	20/30	40-45	50-51	66-71	92-95	95-101
INSTANTANEOUS BANDWIDTH (GHZ)	2	2	2	2	2	2
NOISE FIGURE (DB)	6.5 (6.0)	7.5 (6.0)	8.5 (6.0)	8.5 (6.0)	9.5 (7.0)	10 (7.0)
RF/IF GAIN (DB)	←		20 (25 MIN)			→
L.O. DRIVE (DBM)	←		+5 (+5)			→
DC INPUT CURRENT @ +15V (MA)	←		30 (30)			→

2-25

mounted in a folded Hybrid Tee. The diodes are in an unpackaged configuration and assembled in a modified sharpless wafer mount. The preamplifiers used with these mixers have a typical noise figure of 3 dB and a variety of bandwidths ranging from 100 MHz to 2 GHz.

Present development in the down converter area is in the area of GaAs Schottky barrier diodes and wide band mixers. A broad-band second-harmonic mixer* has been developed to produce 14.6 dB conversion loss over the frequency range of 76 to 106 GHz with an IF of 1.7 GHz.

The millimeter-wave mixer preamplifier can be seriously considered for space use since representative units at 38 and above 50 GHz have already been used in satellite systems.

The long term development for the mixer-preamplifier will be in the area of diodes. GaAs Schottky diodes will produce conversion loss improvements to almost the 4 dB theoretical limit**-***. Full waveguide bandwidths are expected to be achieved along with some major advances in integrated circuits.

2.3.1 SUPERCONDUCTING SCHOTTKY MIXER

The super Schottky diode is a variation of the latter, which employs a superconducting metal contact to a heavily doped semiconductor. This diode operates at cryogenic temperatures and obeys the same equations as the conventional Schottky for voltages up to the superconducting energy gap voltage $(\sim 10^{-3} \text{V})$. The diode exhibits an ideality factor of 1 and a diode noise temperature close to the cryogenic bath.

---

*R. Kawasaki and M. Akaike, "A Broad-Band Second-Harmonic Mixer Covering 76-106 GHz", IEEE Transactions on Microwave Theory and Tech, Vol. MTT-26, pp 425-427, June 1978.

**A.J. Kelly, "Fundamental Limits on Conversion Loss of Double Sideband Resistive Mixers", IEEE Transactions on Microwave Theory and Tech, Vol. MTT-25, pp 867-869, Nov. 1977.

***M. McColl, "Conversion Loss Limitation on Schottky Barrier Mixers", IEEE Transactions on Microwave Theory and Tech, Vol. MTT-25, pp 54-59, Jan. 1977.

Under these conditions the receive noise temperature is given by

$$T_R = L_c T_D + L_c T_{IF}$$

where

L_c is the conversion losses

T_D and T_{IF} the diode and IF noise temperatures

It is possible then, to achieve noise temperatures of the order of tens of ^{O}K, however, the Super Schottky mixer is limited to signal powers of the order of the LO or -50 dBm.

2.3.2 JOSEPHSON JUNCTION MIXERS

A Josephson junction is a superconducting tunnel diode, which can be operated as a low noise mixer over very wide frequency spectrum at mm and sub-mm waves, with very small LO power. Noise temperatures from 3 to $5^{O}K$ are theoretically achievable at the bands of interest, however, saturation occurs at -80 dBm.

2.3.3 VERY LOW NOISE RECEIVERS AT MM WAVES

At mm waves, quantum noise may become a factor as given by Planck's formula:

$$S_n = \frac{hf}{\epsilon^{\frac{hf}{kT}} - 1}$$

where:

S_n spectral noise power density $\left[W/Hz\right]$

h   Planck's constant

f   frequency in Hz

k   Boltzman constant

T   temperature in ^{O}K

2-27

This expression is plotted in Figure 2-17 as a function of frequency for different noise temperatures. It is seen that for the frequency bands of interest and with the exception of very low temperatures, the noise spectral density is constant and given by the Rayleigh-Jeans approximation

$$S_n = kT \qquad for \qquad kT \gg hf$$

Even for the case of the cryogenically cooled, very low noise receivers above discussed, quantum noise is not likely to play a significant role at the frequencies considered in this study, as illustrated by the noise temperatures presently achievable and shown in Figure 2-18.*
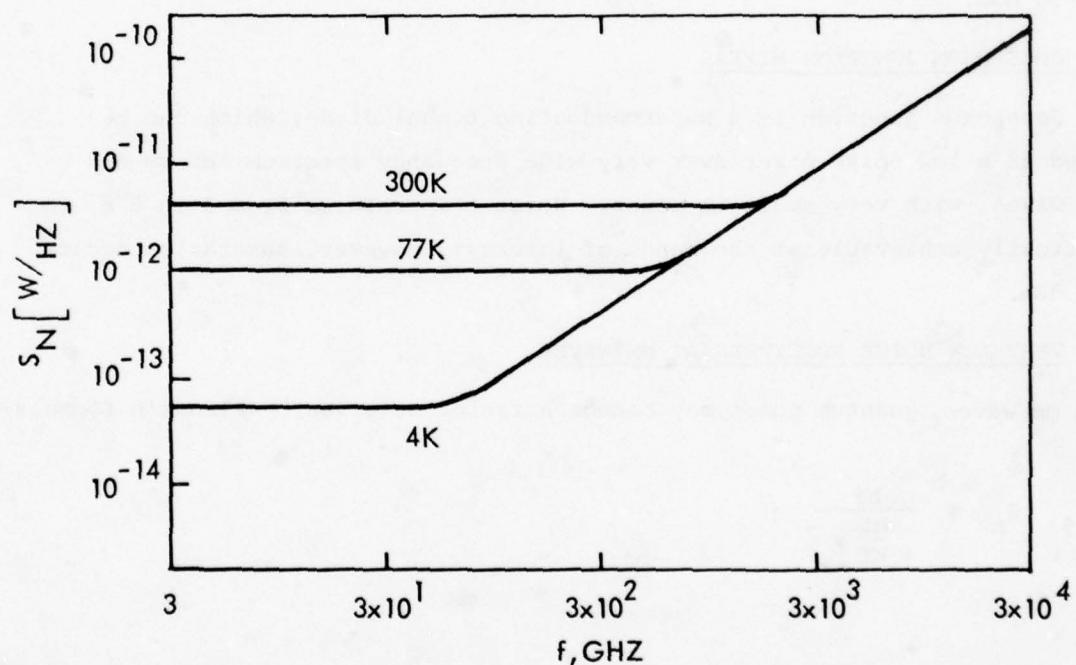
Figure 2-17.   Noise Density At mm Wave Frequencies

---

*A. Silver & T. Hartwick, "New Horizons in Receiver Technology".
The Aerospace Corp.
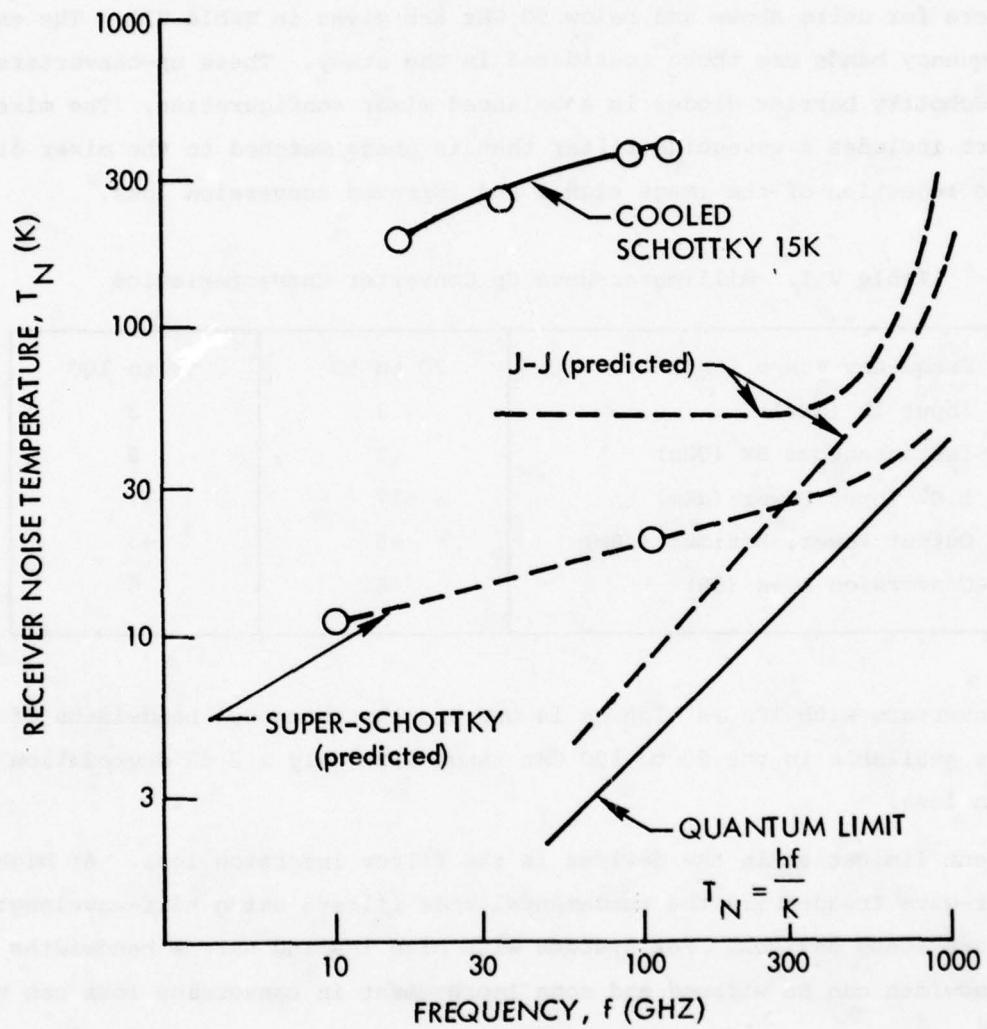
Figure 2-18.   Very Low Noise Temperature mm Wave Receiving Systems

2.4 UP-CONVERTERS

The investigation of up-converter, both high and low level, shows that consistant performance can be achieved across the 20 to 100 GHz frequency range with a family of image rejection mixers. The typical characteristics of the upconverters for units above and below 50 GHz are given in Table VII. The exact input frequency bands are those considered in the study. These up-converters use GaAs Schottky barrier diodes in a balanced mixer configuration. The mixer output port includes a waveguide filter that is phase matched to the mixer diodes to produce rejection of the image signal and improved conversion loss.

Table VII.   Millimeter-Wave Up Converter Characteristics

Frequency Range (GHz)	20 to 50	50 to 100
Input IF (GHz)	3	3
Instantaneous BW (GHz)	2	2
L.O. Input Power (dBm)	+17	+17
Output Power, Maximum (dBm)	+5	+3
Conversion Loss (dB)	6	6

Upconverters with IFs as high as 14 GHz and instantaneous bandwidths of 10 GHz are available in the 50 to 100 GHz range with only a 2 dB degradation in conversion loss.

Present limitation in the devices is the filter insertion loss. At high millimeter-wave frequencies the fundamental mode filters using half-wavelength cavities are lossy devices. For systems with high IFs and narrow bandwidths the filter bandwidth can be widened and some improvement in conversion loss can be realized.

Long term projection for these upconverters forecasts only minor improvements in the current performance. The devices already use GaAs which has the 4 dB theoretical conversion loss minimum stated in the down converter discussion. The major emphasis is being planned in the area of integrated circuits. With further

development in the transmission line area the mixer and possibly the filter could easily be assembled on substrates. Projection of conversion loss in an integrated circuit could not be obtained although it is expected to be higher than the waveguide units.

2.5 MODULATORS

Direct digital modulation at mW Waves is a requirement for achieving Gigabit data rates. These devices use circulator coupled path length modulators to provide a phase change of the signal passing through. Biphase modulation is obtained by 180° phase change and quadriphase by arrangement of biphase modulators as shown in Figure 2-19.*

Either PIN diodes or varactors are used to switch impedances, but the former result in realizations of higher Q's and lower insertion losses. The characteristics of commercially available (Hughes) PIN diode 180° modulators useful over the bands of interest are given in Table VIII.
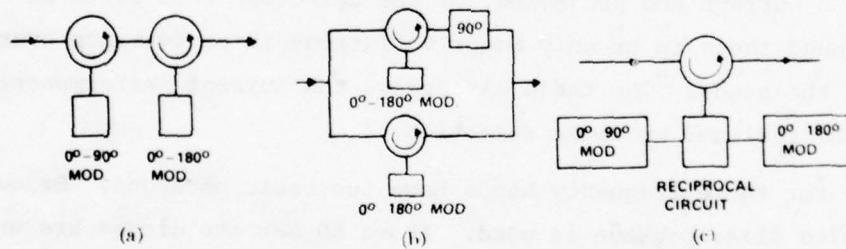
Figure 2-19. Quadriphase Modulator Configurations
(a) Series-connection configuration.
(b) Parallel-connection configuration.
(c) Single circulator-reciprocal circuit configuration.

*Y. Chang, H. Kuno, D. English "High Data Rate Solid State mm Wave Transmitter Module", Transactions MTT-23, June 1975

Table VIII. PIN Biphase Modulators

RF bandwidth	4%
Power handling	100 mW
Switching time (10 to 90%)	500 p sec
Mod rates	>1 Gb/s
Differential phase error	±7°
Insertion loss	Ka 2 dB
	Q 2.5 dB
	V 3 dB
	W 3.5 dB

2.6 DETECTORS

The majority of millimeter wave detectors in today's systems use silicon
Schottky barrier diodes in configurations that mount directly into waveguide.
Fixed-tuned mounts, with replaceable diodes, achieve good sensitivity across the
full waveguide bandwidth which eliminates the cumbersome mechanical tuning for
system optimization at frequencies above 40 GHz. Table IX gives the typical
performance, both current and projected, of the detectors from 20 to 100 GHz.
Diode vendors found there to be only minor variations in performance over the
80 GHz range of the study. The table also shows the current performance improve-
ments that can be realized by diode selection.

The diodes for these frequency bands have two basic packages. Below 50 GHz
a miniature sealed glass package is used. Above 50 GHz the diodes are unsealed
and mounted in an improved sharpless-type wafer. Both types are rugged enough
for satellite application since the size and mass of the diode are very small
and the mount, securing the diode, is a very simple mechanical structure.
Similar diodes have already been used aboard satellite systems operating at
38 and above 50 GHz.

The major long-range development in millimeter-wave diodes will be in the
area of the zero-bias Gallium Arsenide (GaAs) Schottky barrier diode. The
zero-bias Schottky will produce simple and stable detector circuits that are

Table IX. Current Millimeter-Wave Detector Performance

	Typical	Selected
Bandwidth	±1.5 dB over Full Waveguide Bandwidth	
Tangential Sensitivity (1 MHz Video Bandwidth)	-50 dB	-55 dB
Sensitivity (mv/mw)	300	900
Saturation Level (mw)	100	100
VSWR	2:1	2:1

presently available at X and Ku-bands. The GaAs with its higher electron
mobility will give an improvement in 1/f video noise performance and have typical
characteristics of the selected Schottky diodes of Table IX.

2.7 POWER MEASURING DEVICES

RF power can be measured in a variety of ways at any of the bands of interest.
They include

- crystal detectors
- bolometers
- thermistors
- calorimeters
- water load with integral thermopile

The crystal detector is a well known technique used in many operational
systems where the diode output voltage can be sampled and power determined from
a calibration curve. The crystal detector method is generally restricted to the
diode square-law region which has a typical upper limit of -10 dBm. The detector
sensitivities of Table IX of Section 2.6 apply to this technique.

The bolometer, a conductor with a positive temperature coefficient of
resistance, and the thermistor, a semiconductor with a negative temperature
coefficient of resistance, are also well known components that are generally
used as testing power measuring standards. They are also restricted to laboratory
environment because of the temperature compensation circuits needed for stable

2-33

measurements. The maximum power handling of these two devices is +10 dBm. The minimum power measured is -20 dBm and is severely limited by the meter drift associated with the discrete elements and the temperature compensation circuits. Another limitation of these devices at millimeter-wave frequency is the accuracy. The typical efficiency at 45 GHz and 94 GHz is 80 and 60%, respectively. Improvements in efficiency are already being made with bolometers using a distributed bolometer element.* Continued improvement in efficiency and thermal drift are expected over the next 10 years to get the thermistor and bolometer type power meters to the refined level of current devices at X and Ku-band frequencies.

Calorimeters, both dry and wet type, are presently the most accurate method of measuring RF power at millimeter-wave frequencies. The device is capable of measuring power levels from 100 μwatts to 0.5 watts with an accuracy of better than 5%. The calorimeter method is used exclusively in the laboratory environment as a secondary type power measuring standard. The devices are never used in operational systems because of their large size and response time, which is typically 60 seconds. No dramatic improvement in this device is planned since the accuracy of 5% is sufficient for most systems.

The water load with integral thermopile is really a variation of the wet type calorimeter and is used for RF power levels in excess of 1 watt. The water cooled load can be selected for different frequency bands and different power levels. The device does not have the accuracy of the calorimeter because of the lack of high power calibration standards. The current accuracy is less than 10%.

*T. Inone and T. Nemoto, "High-Efficiency Millimeter-Wave Bolometer Mount", IEEE Transaction Microwave Theory Tech., Vol. MTT-25, pp 694-697, Aug. 1977.

2-34

SECTION 3

TUBES

Suitable devices for power generation at frequencies above 20 GHz include travelling wave tubes (TWT), klystrons, cross field devices and gyrotrons. The selection of a particular type depends on required power level, bandwidth, waveform etc., and is discussed below per separate for ground and space application.

3.1 GROUND APPLICATIONS

The state of the art in power output capability for different tube technologies, as a function of frequency, is illustrated in Figure 3-1*. A graph of conventional tubes above 30 GHz, currently available, is shown in Figure 3-2.
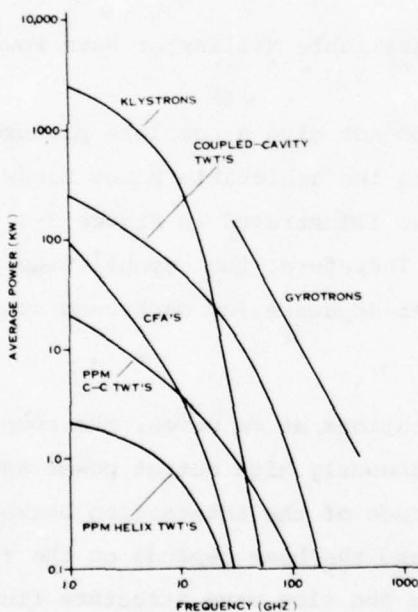
Figure 3-1. Average Power Capability of Various Microwave Tubes

*A. Strapans "High Power Microwave Tubes" 1976 International Electron Devices Meeting, Washington, D.C.
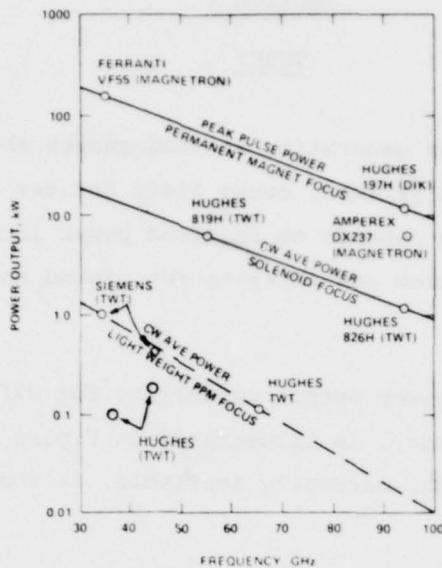
Figure 3-2.   Available Millimeter Wave Power Tubes

These figures, however, do not give a complete picture of the device output
power limitations in regards to the achievable power bandwidth product. The latter
is another design trade off, as illustrated in Figure 3-3 for a 44 GHz, PPM coupled
cavity travelling wave tube. Therefore, the capabilities and limitations of each
device have to be addressed per separate for each band specific requirements.

3.1.1   COUPLED CAVITY TWT

For communications applications at mm waves, the coupled cavity TWT is the
device used to achieve simultaneously high output power and wide bandwith. In a
coupled cavity TWT, the magnitude of the interaction between the wave propagated
over the slow wave structure and the beam depends on the filling factor of the beam
passage of the cavities, since the slow wave structure field decreases substan-
tially at a small fraction of wavelength away from the metal structure. There-
fore, a reasonable coupling at mm waves will result in extremely high beam density,
and stringent mechanical tolerances. Good focussing must be achieved to maintain
low intercept current since poor beam transmission will limit the maximum allow-
able beam current, and, therefore, the output power obtainable without outgassing
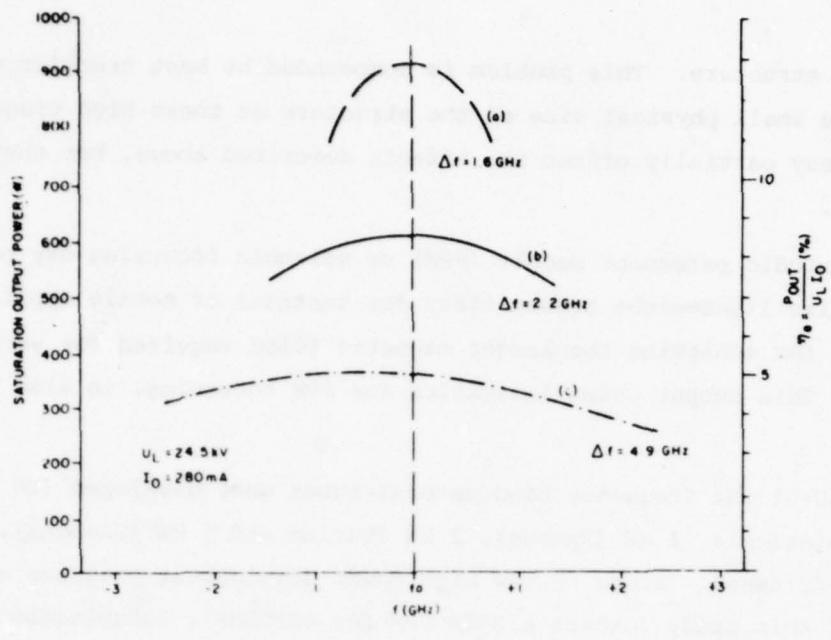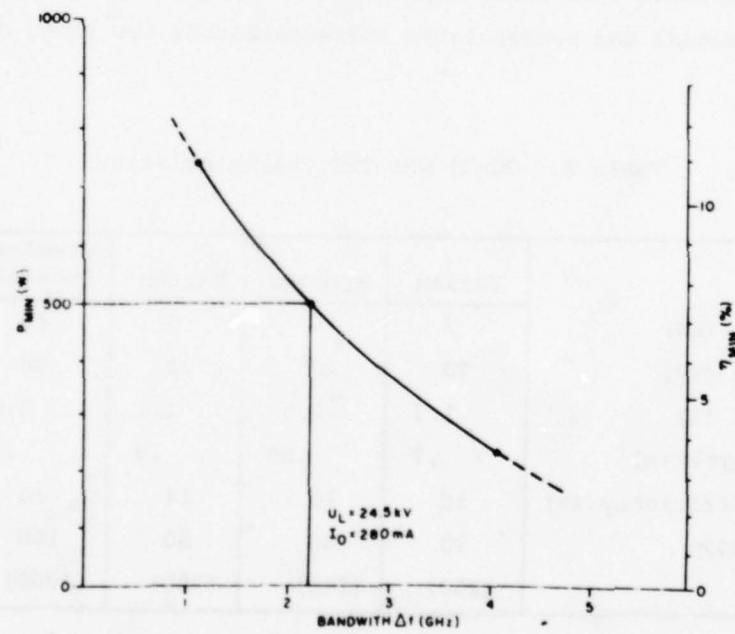
Figure 3-3.   Power-Bandwidth Tradeoff for PPM Focused Coupled Cavity TWT

or melting the structure. This problem is compounded by heat transfer difficulties due to the small physical size of the structure at these high frequencies. High voltages may partially offset the effects described above, but they introduce other problems.

Either periodic permanent magnet (PPM) or solenoid focussing may be used, the former to realize lightweight transmitters for tactical or mobile applications and the latter for achieving the larger magnetic filed required for very high output power. This output power limitation for PPM focussing, is also illustrated in Figure 3-2.

For the 30-31 GHz frequency band several tubes were developed (to different states of completion): 1 kW (Hughes), 2 kW (Varian and 5 kW (Siemens), all of them solenoid focussed. Since no new high power development programs are active at the time of this study (except a 250W PPM for SATCOMA), consultation was held with Varian and Hughes engineering organizations to assess the state-of-the-art at both companies. Although Siemens was not consulted due to classification reasons, it is estimated that similar performance may be attainable with their technology. The actual and extrapolated characteristics for these devices are shown in Table X.

Table X. 30-31 GHz TWT Characteristics

	Varian	Siemens	Varian	Siemens (Scaled)	Hughes
Output Power (kW)	2	5	5	10	22
Beam Voltage (kV)	15	20	22	28	85
Beam Current (A)	1.3	2.5	1.6	3.6	1.23
Permeance (μpervs)	.7	.89	.5	.75	.05
Electronic Efficiency (%)	10	10	14	10	21
Tube Cost (K$)	20	80	50	100	180
NRE (K$)	(250)	(250)	(750)	(1000)	(1400)

The 22 kW tube proposed by Hughes can be considered the ultimate performance that may be obtained from coupled cavity TWT's at this band. Very low perveance allows to realize large coupling impedance, as reflected by 21 percent electronic efficiency, with very high (99%) beam transmission. The limiting factor is in this case heat transfer due to the RF losses in the slow wave structure.

The 10 kW tube data has been obtained by direct scaling the 5 kW Siemens design and preserving the same focussing axial field.

For the 43-45 GHz band, the only high power device available at present is a 500W PPM focussed tube shown in Figure 3-4 (Raytheon/Siemens), covering the entire 43-45 GHz (4.6 percent) band. Higher output power may be obtained from solenoid focussing or by trading output power for instaneous bandwidth as shown in Figure 3-3. The scaling of the above tube design for solenoid focussing and narrower instaneous bandwidth is shown in Table XI. In addition, Varian and Hughes were consulted regarding their technological capabilities for high power devices at these frequencies, and their inputs are also shown in Table XI.
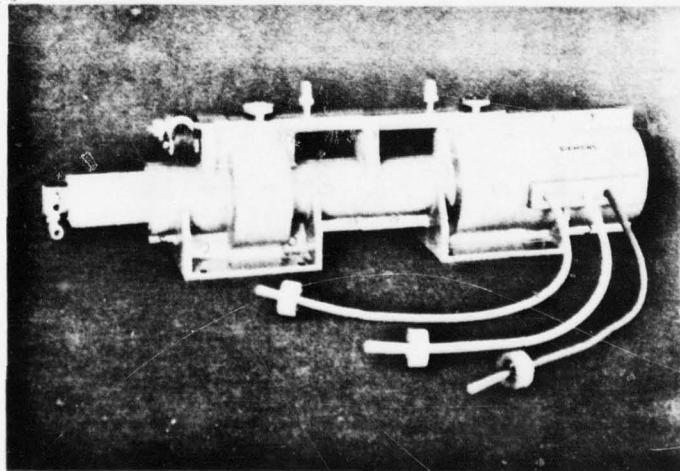
Figure 3-4. 500W PPM Coupled Cavity Q Band TWT

Table XI. Q-Band TWT Characteristics

	Siemens	Siemens	Siemens	Varian	Siemens (Scaled)	Hughes	Hughes
Output Power	500W	900W	1 kW	2.5 kW	5 kW	10 kW	14 kW
Focussing	PPM	PPM	Solenoid	Solenoid	Solenoid	Solenoid	Solenoid
Instantaneous Bandwidth (GHz)	2	1	2	2	1	2	1
Beam Voltage (kV)	25	25	29	27.5	34	66	72
Beam Current (A)	0.28	0.28	0.48	0.9	1.23	0.8	0.96
Perveance (μ pervs)	0.07	0.07	0.1	0.2	0.2	0.05	0.05
Electronic Efficiency (%)	7	12.6	7	10	12.6	18	10
Depression (%)	40	40	40	50	40	40	40
Tube Cost (K$) NRE (K$)	80 -	80 (100)	80 (250)	50 (750)	100 (500)	200 (1900)	200 (1900)

The 10 and 14 kW tubes proposed by Hughes can be considered as the ultimate performance obtainable from coupled cavity TWT's in this band. It is obtained with very low perveance, which maximizes the coupling impedance and therefore the electronic efficiency and beam transmission (99 percent). Electronic efficiencies up to 15 percent have been experimentally obtained at Hughes in a PPM design at low powers. The tubes would also require elaborate multiple step velocity tapers in the output section. Limiting factor in achieving this larger power will again be the heat transfer problems due to rf losses in the last section of the slow wave structure.

The 1 and 5 kW solenoid focussed tubes listed in Table XI are the scaled version of the Siemens PPM designs and allowing for the increased beam density possible with solenoid focussing capable of 4K gauss axial field.

At higher frequencies, a number of experimental tubes were developed by Hughes as shown in Figure 3-2. At 55 GHz, the 819H (Figure 3-5) delivers 6 kW at 30% efficiency and having a 20 dB gain. At 94 GHz the 826H delivers in excess of 1 kW.
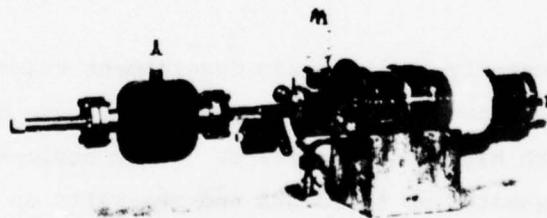
Figure 3-5. The Hughes 819H 55-Gc/s High Power Amplifier. This tube has delivered 6 kW of output power at 30 percent efficiency.

3.1.2 HELIX TWT

Helix tubes may be built at mm waves, however, output power will be limited due to the heat transmission capabilities of the helix structure and due to the fact that the maximum beam voltage is limited by the increase of the helix pitch.

Scaling from existing lower frequency designs using the theoretical scaling law $Pf^{8/3} = K$ result in PPM helix tubes producing 30W at the 30-31 GHz band. More on helix tubes is discussed below in connection with space tubes.

3.1.3 KLYSTRON

Klystrons may be used as oscillators or amplifiers at mm waves. The former have traditionally been used as pumps in parametric amplifiers, but they are currently being replaced by solid state sources.

Klystron amplifiers at mm waves are intrinsically narrowband devices which in general will not be suitable for wideband communication systems. For instance, a 1 kW klystron at 36 GHz developed by Varian exhibits a 30 MHz bandwidth.

3.1.4 MAGNETRONS AND CFA

Magnetrons are being used as pulse power sources in mm wave Radars and are currently available in the bands of interest as shown in Figure 3-2. However, there is little hope of realizing the CW efficiency advantages of Cross Field Amplifiers (CFA) at frequencies much beyond X-band.

3.1.5 GYROTRONS

Gyrotron devices presently in the basic development stage, will in the future, be able to generate mm wave power levels comparable to those obtainable at lower microwave frequencies with klystrons and TWT's. These devices have shown the potential to generate gigawatts up to 10 GHz and megawatts up to 100 GHz. In this general category are, in the addition to the gyrotron, up converters using the reflection of electromagnetic energy from relativistic beams.

The gyrotron, also known as Cyclotron Resonance Maser (CRM), may operate with intense relativistic beams or conventional tube voltage and currents. The CMR employs a cloud of mono energetic electrons, usually generated by a magnetron injection gun (MIG), to launch an annular beam with large transverse energy and minimum spread into either a cavity or a fast wave structure. Initially the

phases of the electrons in their cyclotron orbits are random, but phase bunching can occur because of relativistic mass change of the electron. This bunching has much in common with conventional tubes and result in similar structures as shown in Table XII*. This table shows the theoretical efficiency at the fundamental gyro resonance, but also high efficiency is possible at harmonics as shown in Table XIII. High intensity magnetic fields are required in general for these devices, but being lower for harmonic operation. For the later case conventional electromagnets are adequate, but superconductive magnets are also commonly used.

Table XII. Possible Gyrotron Configurations

"O" TYPE DEVICE	MONOTRON	KLYSTRON	TWT	BWO	TWYSTRON
TYPE OF GYROTRON	GYRO-MONOTRON	GYRO-KLYSTRON	GYRO TWT	GYRO BWO	GYRO-TWYSTRON
RF FIELD STRUCTURE					
ORBITAL EFFICIENCY	0.42	0.34	0.7	0.2	0.6

Table XIII. Monotron Efficiency at Gyroresonance Harmonics

n	1	2	3	4	5
$\eta_\perp$	0.42	0.30	0.22	0.17	0.14

Some peak power levels obtained by intense relativistic electron beams through the CRM process are given in Table XIV**. These powers were short pulses generated from cold field emission cathodes, showing high degree of temporal and spatial coherence.

*V. Flyagin, A. Gapanov, M. Petelin, V. Yulpatov "The Gyrotron" Transactions MTT-25, June 1977.
**T. Godlove, V. Granatstein "Gyrotron, Reborn Tube" Microwave Systems News, Nov 1977.

3-9

Table XIV. Peak Power Levels from Cyclotron Masers Driven by
Intense Relativistic Electron Beams

Wave-length (cm)	Peak Power (mw)	Diode Voltage (MV)	Diode Current (kA)
4	900	3.3	80
2	350	2.6	40
0.8	8	0.6	15
0.4	2	0.6	15

Table XV shows the experience accumulated to date on devices using thermo-ionic cathode guns. The Soviet experiments have produced 22 kW at 150 GHz and 1.5 kW at 326 GHz monotrons. Varian is working in a multicavity gyroklystron at 28 GHz and NRL a gyro TWT to achieve 280 kW peak at 35 GHz.

Table XV. CRM Devices Operated or Being Designed

λ (mm)	P(kw) gain	n	Tube Type	Eff (%)	Gun Type	B (kG)	Mag-net	V/I (kV/A)	Mode (TE)
20	4	1	GM	50	MIG	5.4	Std	20/0.3	011
12	4.5	2	GM	16	MIG	4.5	Std	20/1.5	021
8.9	9	2	GM	40	MIG	6.0	Std	19/1	021
8.9	(40)	2	GM	43	MIG	6.0	Std	25/3	021
2.8	12	1	GM	31(36)	MIG	41	S.C.	27/1.4	021
1.9	2w	2	GM	10(15)	MIG	29	S.C.	18/1.4	031
2.0	7	2	GM	15(20)	MIG	29	S.C.	26/1.8	231
0.9	1.5	2	GM	6(5)	MIG	61	S.C.	27/0.9	231
1-2	(1μw)	1	GM		Triode	100	Std	10/0.05	over
2-4	(1w)	1,2	GM	2	Pierce	50	S.C.	20/	over
46	30μw	1	GK			2.3	Std	1-5/	TM_{010}
30	10dB	2	GK		MIG	2.0	Std	40/4.5	011
3.2	(10-100)	4	GT		MIG	9.0	Std		
8	(300) 20dB	1	GT	(53)	MIG	13	S.C.	70/8.3	01
8	200	1	GM		MIG	13	S.C.	70/8.3	011 111
1.3	1-10	2-4	GM		MIG	< 50	S.C.		
11	(25) 20dB	1	GK	(44)	MIG	11	Std	80/8	01/02
11	(250)	1	GM	34(37)	MIG	11	Std	80/9	021

Notes:
a. pulsed power in parentheses; otherwise cw; b. harmonic number; c. GM = gyromono-tron, GK–gyroklystron, GT = gyro–traveling–wave–amplifier; d. experimental (theoretical); e. MIG = magnetron injection gun; f: Std = normal electromagnet, S.C —superconducting magnet.
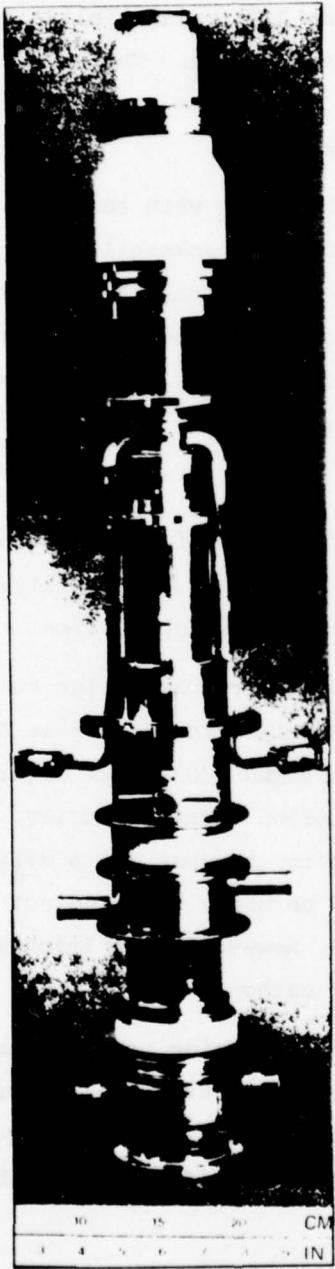
Figure 3-6. 28 GHz Gyroklystron

Varian has built a single cavity gyroklystron oscillator which produced 248 kW at 28 GHz, with a 80 kV beam pulsed at 9A, with a 4% duty factor, in a 11 kG conventional magnetic field. The conversion efficiency was 35%. They are building a two cavity klystron (Figure 3-6) using similar techniques to have a small signal gain of 38 dB, 30 dB at saturation. The output has been limited due to spurious oscillations, which is one of the current technical problems in the gyrotron evolution to be overcome.

The estimated bandwidth achievable with this device will be 0.1% for gyroklystron and 3% for gyro TWT, with the possibility to extend it to 10%. Another feature of the gyrotron is that the resonant frequency is determined by the magnetic field rather than physical dimension of the resonant or fast wave structure, and electronic tunability is possible. For a gyro TWT the tuning range is estimated from 5 to 10% and possible 20 to 30%.

3.2 SPACE APPLICATION**

As discussed above, the TWT amplifier is the ideal device for medium power output at mm waves, and both helix and coupled cavity tubes are likely candidates for downlink spacecraft power amplifier application.

For a space application the major tube design considerations are life and efficiency. In most TWTA the lifelimiting factor is the cathode. For conventional space tubes, lifetime of more than 100000 hrs is obtained from oxide coated cathodes at low temperatures and low emission current density. For higher frequency and power, the emission density has to increase and a different type such as dispenser or impregnated cathodes have to be used, which do not have the known record on the oxide cathodes. It is believed, however, that lifetimes in excess of 5 years will be obtained with these types of cathode.

Because of the usual weight and prime power restrictions in spacecrafts, higher efficiencies are very desirable, which are obtained by depressed collector operation and by multistage collectors. The later technique has to be traded against the additional complexity and loss of efficiency of the power conditioner. Also,

---

**T. H. Herman "TWT Amplifiers above 10GHz for Space Application" ATAA/CASI 6th Communication Satellite Systems Conference Montreal, 1976

weight and volume of the power conditioner is a function of the operating voltages which tend to favor helix tubes when the possibility of using both design techniques is feasible.

3.2.1 HELIX TWT

A variety of devices have been developed up to 40 GHz as indicated by Figure 3-7. The upper zone of the figure shows a tentative power/frequency upper limit.
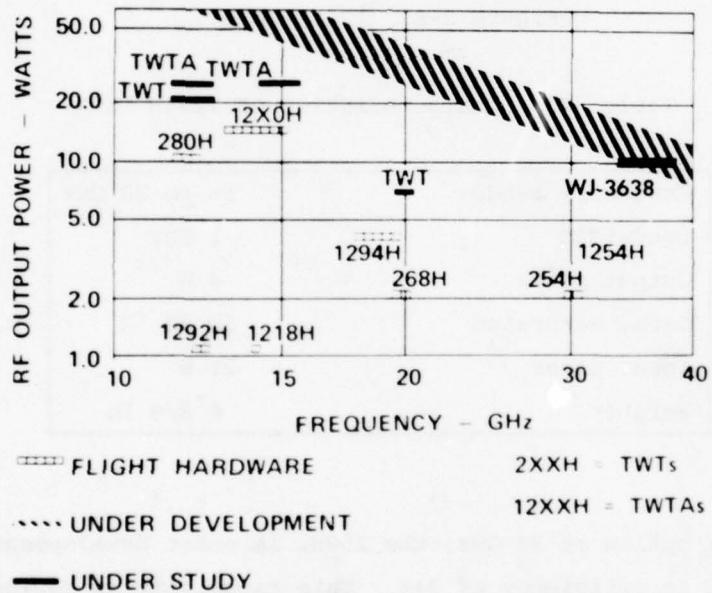
Figure 3-7. Helix Traveling Wave Tubes and Amplifiers

At 20 GHz, Hughes has developed 4W TWTA for the Japanese Communication Satellite. This tube is an outgrow of the tube developed for the ATS program and the power conditioner is a modification of the one used in the RCA SATCOM program providing 85 to 90% efficiency. The TWTA is shown in Figure 3-8 has the characteristics given in Table XVI.

3-13
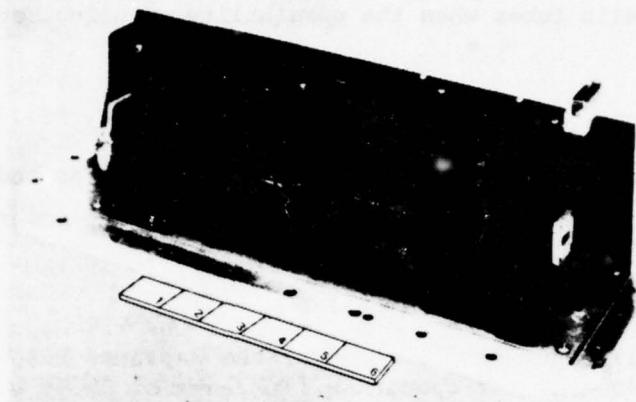
Figure 3-8. 1294H TWTA

Table XVI. Characteristics of 1294H TWTA

Frequency range	18 to 20 GHz
Bandwidth	1 GHz
Output power	4 W
Gain, saturated	50 dB
Input power	21 W
Weight	4 3/4 lb

A higher power option at 20 GHz, the 250H, is under development and has demonstrated 30W at an efficiency of 34%. This capability is designed as a booster for intermittent operation to overcome rain attenuation, and therefore at high current density, which is reduced for normal operation at lower output levels.

At 40 GHz, Watkins Johnson has a 10W tube under development and having the characteristics of Table XVII and shown in Figure 3-9.

3.2.2 COUPLED CAVITY TWT

As the operating frequency increases, there are fundamental limitations in realizing helix TWT's and the coupled cavity slow wave structures become more

3-14

Table XVII.   Characteristics of WJ-3638 TWT

Frequency Range	26-40 GHz
Bandwidth	3 GHz Bandwidth
Output Power	10 W
Gain	25 dB
Efficiency	20%
Weight	2.5 lbs
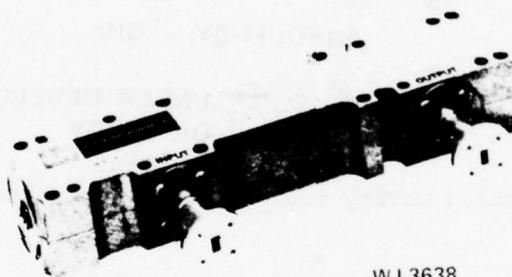
WJ-3638

Figure 3-9.   Watkins Johnson 10w Tube-WJ-3638 TWT

appropriate. Coupled cavity tubes have been developed for space applications only recently, however is an active field in US and Europe, in connection to programs to obtain the high output power required for satellite TV distribution. Figure 3-10 shows coupled cavity tubes available and under development at mm wave frequencies.

At 40 GHz, a 100W tube having a bandwidth of more than 2 GHz has been demonstrated by Hughes. This tube has an efficiency approaching 25%.

At 60 GHz, a TWTA providing 13W (Figure 3-11) has been tested through qualification level of tests. Because of the high operating voltage (13kV) this assembly is oil immersed, as well as the gun and collector areas of the tube.

3-15
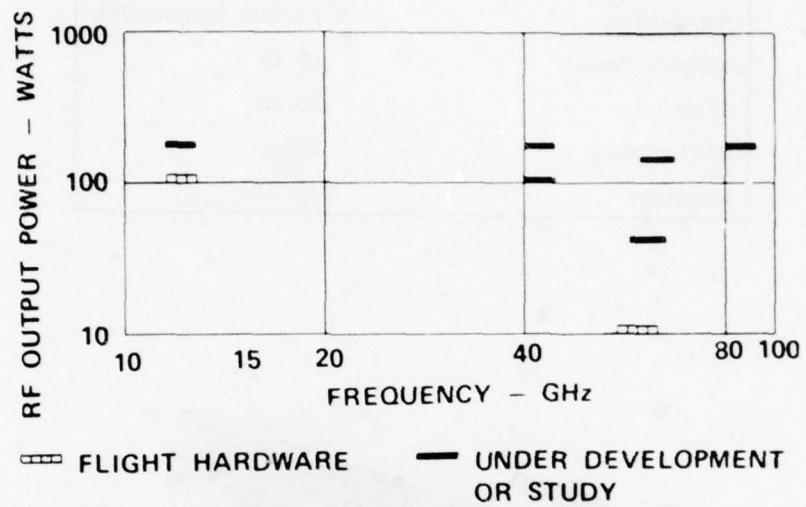
Figure 3-10. Coupled Cavity Traveling Wave Tubes and Amplifier
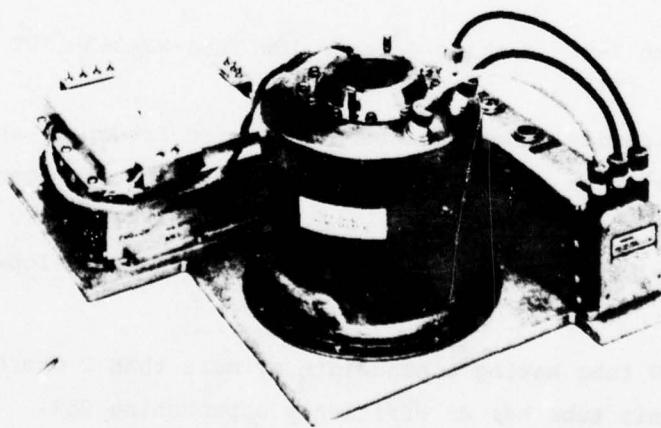
Figure 3-11. 60-GHz TWTA

3-16

With a single depressed collector the tube operates at 24% efficiency and the power supply at 65%. The characteristics of this TWTA are given in Table XVIII.

Table XVIII. Characteristics of 60-GHz TWTA

Output power	13 W
Bandwidth	1%
Gain, saturated	40 dB
Noise figure	28 dB
AM/PM conversion	10 deg/dB
Efficiency	13%
Weight	50 lb

Based on this amplifier, feasibility models have been developed for 50W and 100W. The 50W tube (Figure 3-12) operates at 18% overall efficiency, including power supply, with 55 dB gain and has also undergone qualification tests. The 100W tube has a velocity taper and two depressed collector stages, resulting in 30% efficiency at 1.2% bandwidth and an overall TWTA efficiency of 24%.
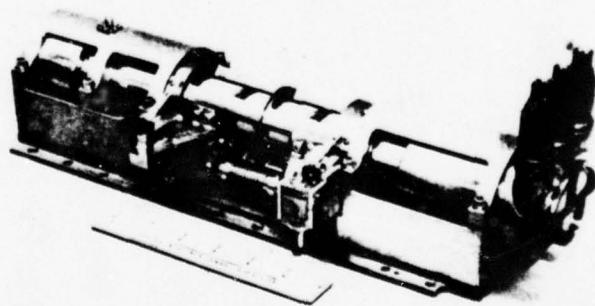
Figure 3-12. 50-W 60 GHz Traveling Wave Tube

SECTION 4

TRANSMISSION COMPONENTS

Transmission components suitable for the mm wave bands considered in this study may be implemented with small semirigid coaxial cable and cavities, rectangular and circular waveguides and cavities, and Microwave Integrated Circuit (MIC) techniques, as shown in Figure 4-1. The typical parameters and the comparison at different frequencies, are given in Table XIX.[*]

This section addresses to these transmission media and discusses some of the passive components that can be realized.

4.1 WAVEGUIDE

Waveguide is the preponderant media for realizing active and passive components and subsystems at mm waves. Both rectangular and circular waveguides and cavities are commonly used at these frequencies.

Table XX gives the standard rectangular waveguides used in the frequency bands of interest of this study.[**] Due to the appreciable losses at these frequencies, circular waveguide is used for long runs and outweigh the additional complexities of mode launchers, suppression, etc. A comparison between rectangular and circular waveguide at 30 GHz is given in Table XXI.

The circular waveguide low loss modes do not exist without potential problem areas. The main problem is the existence of extraneous modes. In general, the waveguide insertion loss is inversely proportional to the wall circumference, the larger the waveguide the lower the loss. The increased size, however, lowers the cutoff frequency and permits other modes to propagate in the guide. The TE_{01} mode presents the biggest mode problem since the generally chosen guide diameter is the largest possible without propagating the troublesome TE_{02} mode. This choice of

[*]M. Jacobs "mm Wave integrated circuits" ARPA - Tri Service mm Wave Workshop, Johns Hopkins University, Dec 1974.
[**]Microwave Journal "Microwave Engineers Technical and Buyers Guide"

NON-TEM LINES
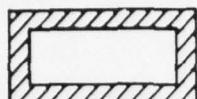
WAVEGUIDE

IMAGE LINE

SLOT LINE
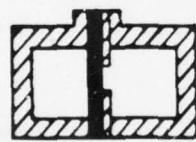
FIN LINE

DIELECTRIC WAVEGUIDE
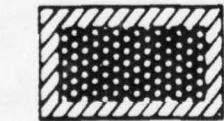
DIELECTRIC FILLED WAVEGUIDE

MICROGUIDE

TEM AND QUASI-TEM LINES

COAXIAL LINE

MICROSTRIP
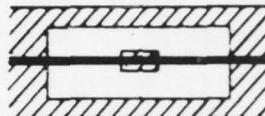
BALANCED SUSPENDED STRIPLINE
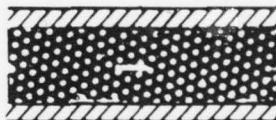
DIELECTRIC LOADED STRIPLINE
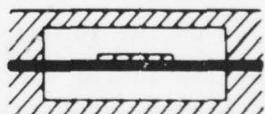
UNBALANCED SUSPENDED STRIPLINE

COPLANAR WAVEGUIDE

TRAPPED INVERTED MICROSTRIP

PARALLEL PAIR PLANAR

Figure 4-1. Various Microwave Transmission Media Listed by Mode

4-2

Table XIX. Characteristics of Transmission Lines

	Rectangular Waveguide TE_{10} Mode	Coaxial Line Ten Mode $\epsilon_r = 1$	Microstrip $\epsilon_r = 3.8$ $\epsilon_{eff} = 2.98$	Balanced Stripline $\epsilon_f = 3.8$	Dielectric Waveguide Silicon
10 GHz, Z in ohms	444	50	50	50	109
10 GHz, λ_g in cm	3.98	3	1.75	1.54	.87
10 GHz, α dB/m	.108	.340	2.65	489	2.05 – .64 10^4 ohms cm to 3×10^4 ohms cm
10 GHz, Q	6330	2650	594	363 (720, ϵ_f =1)	630 – 1890 Exp.> 900 (Al_2O_3)
60 GHz, Q	2560	1080	242	148 (280, ϵ_f =1)	3690 – 11,300

Table XX.   mm Wave Standard Rectangular Waveguide

EIA WG Designation WR( )	Recommended Operating Range for TE10 Mode Frequency (kmc/sec)	Wavelength (cm)	Cut-off for TE10 Mode Frequency (kmc/sec)	Wavelength (cm)	Range in 2λ/λc	Range in λg/λ	Theoretical cw power rating lowest to highest frequency megawatts	Theoretical attenuation lowest to highest frequency (db/100 ft.)	Measured Alloy	JAN WG Designation RG ( )/U	JAN FLANGE DESIGNATION Choke UG( )/U	Cover UG( )/U	EIA WG Designation WR( )	DIMENSIONS (inches) Inside	Tol.	Outside	Tol.	Wall Thickness Nominal
51	12.00-22.00	2.00-1.36	11,574	2.590	1.54-1.05	1.59-1.18	0.030-0.107						51	0.510-0.255	±.0025	0.570-0.375	±.003	0.010
42	17.00-25.50	1.66-1.13	14,047	2.134	1.56-1.06	1.60-1.18	0.043-0.058	20.7-14.8 Brass / 17.6-12.6 Alum. / 13.3-9.5 Silver		53 / 121 / 66	596 / 598 / —	595 / 597 / —	42	0.420-0.170	±.0020	0.500-0.250	±.003	0.010
34	22.00-33.00	1.36-0.91	17,328	1.730	1.57-1.05	1.62-1.18	0.034-0.048						34	0.340-0.170	±.0020	0.420-0.250	±.003	0.010
28	26.50-40.00	1.13-0.75	21,081	1.422	1.59-1.05	1.65-1.17	0.022-0.031	— — / — — / 21.9-15.0 Brass/Alum./Silver	— / — / 96	600 / — / —	599 / — / —	28	0.280-0.140	±.0015	0.360-0.220	±.002	0.040
22	33.00-50.00	0.91-0.60	26,342	1.138	1.60-1.05	1.67-1.17	0.014-0.020	— — / 31.0-20.9 Brass/Silver	— / 97		383 / —	22	0.224-0.112	±.0010	0.304-0.192	±.002	0.040
19	40.00-60.00	0.75-0.50	31,357	0.956	1.57-1.05	1.63-1.16	0.011-0.015						19	0.188-0.094	±.0010	0.268-0.174	±.002	0.040
15	50.00-75.00	0.60-0.40	39,863	0.752	1.60-1.06	1.67-1.17	0.0063-0.0090	— — / 52.9-39.1 Brass/Silver	— / 98		385 / —	15	0.148-0.074	±.0010	0.228-0.154	±.002	0.040
12	60.00-90.00	0.50-0.33	48,350	0.620	1.61-1.06	1.68-1.18	0.0042-0.0060	— — / 93.3-52.2 Brass/Silver	— / 99		387 / —	12	0.122-0.061	±.0005	0.202-0.141	±.001	0.040
10	75.00-110.00	0.40-0.27	59,010	0.508	1.57-1.06	1.67-1.18	0.0030-0.0041						10	0.100-0.050	±.0005	0.180-0.130	±.001	0.040
8	90.00-140.00	0.33-0.21	73,840	.406	1.64-1.05	1.75-1.17	0.0018-0.0026	152-99 Silver	138	—	—	8	0.080-0.040	±.0005	0.160-0.120	±.001	0.040

Table XXI.   30 GHz Losses for Different Modes

	Rectangular		Circular	
	TE10		TE01	TE11
Waveguide Type	WR34	WR28	WRC997D14-A	WRC182C14-S
Dimensions (in.)	1.372 x .622	.28 x .14	.797 ID	.438 ID
Loss (dB/ft)	.12	.18	.014	.046

4-4

diameter permits as many as 14 modes to exist in the guide and for optimum mode suppression the transmission systems used at EHF frequencies may be a combination of TE_{11} and TE_{01} waveguide components. Tables XXII and XXIII give the transmission line characteristics for both modes, at 30 GHz and Q band using standardized circular waveguide. The diameters have been selected to be cut off at the TE_{02} mode for the TE_{01} guide and at the TE_{01} mode for the TE_{11} waveguide. Aluminum, instead of coin silver, may be used in the TE_{01} mode, since the electric field configuration is circular with negligible current in the waveguide walls.

Table XXII. 30 GHz Transmission Line Characteristics

	TE_{01}	TE_{11}
Waveguide Type	WRC997D14-A	WRC182C14-S
Internal Dimensions	.797 Diameter	.438 Diameter
Material	Aluminum	Coin Silver
Insertion Loss, dB/ft	.014	.046
Waveguide Pressure, psi	15	15
CW Power Handling, MW	90	.028
Possible Extraneous Modes	10	1

Table XXIII. Q Band Transmission Characteristics

	TE_{01}	TE_{11}
Waveguide Type	WRC159C14-A	WR283C14-S
Internal Dimensions	.500 Diameter	.281 Diameter
Material	Aluminum	Coin Silver
Insertion Loss, dB/ft	.036	.097
Waveguide Pressure, psi	15	15
CW Power Handling, MW	.035	.011
Possible Extraneous Modes	8	8

4-5

In order to realize a low loss transmission line, free from extraneous modes, with circular waveguides, critical constraints are placed on the path configuration. The path must use the TE_{01} waveguide wherever possible, since it has the lower loss. This waveguide requires an extremely straight run between its mode launchers, in order to prevent conversion to extraneous modes. The TE_{11} waveguide operates much like the rectangular waveguide and is much less sensitive to changes in the path direction. The only precautions for the TE_{11} waveguide are in the bends- where large radii should be used, and in the orientation of the TE_{11} mode launchers, since the electric field is linearly polarized.

For high power applications, the power handling capability of mm Waveguide is substantially lower than their microwave frequencies counterpart. This power capability has to be derated for VSWR, altitude, etc, and may be increased by pressurization. A typical derating is given in Table XXIV.

Table XXIV. EHF Waveguide Power Handling Derating

VSWR, 1.2:1	.82
Altitude, 2500 ft	.80
Cooling Temperature, $60^{\circ}C$	.75
Pressure, Dry Air 30 psiA	2.00
Rotary Joint	.32
Mode Launcher	.65
Mode Suppressor	.50
Bend	.95
Flange	.95
Cumulative Derating	.06

4.1.1 Waveguide Passive Components

The same variety of microwave waveguide passive components such as directional couplers, attenuators, filters, etc, may be realized at the mm wave bands considered here. Figure 4-2 shows a number of Ka-band components developed for ground terminal application in rectangular waveguide and in Figure 4-3 in circular waveguide.

These waveguide components may be fabricated by standard machining methods, but electroforming is gaining popularity for complicated parts and close tolerances.

The typical performance achieved with electroform passive components is illustrated in Table XXV.

For space application these waveguide components may be built with newly developed graphite-epoxy composite materials described in Section 5. These materials result in weights about 1/3 less than when built in aluminum, with one order of magnitude less thermal expansion coefficient.
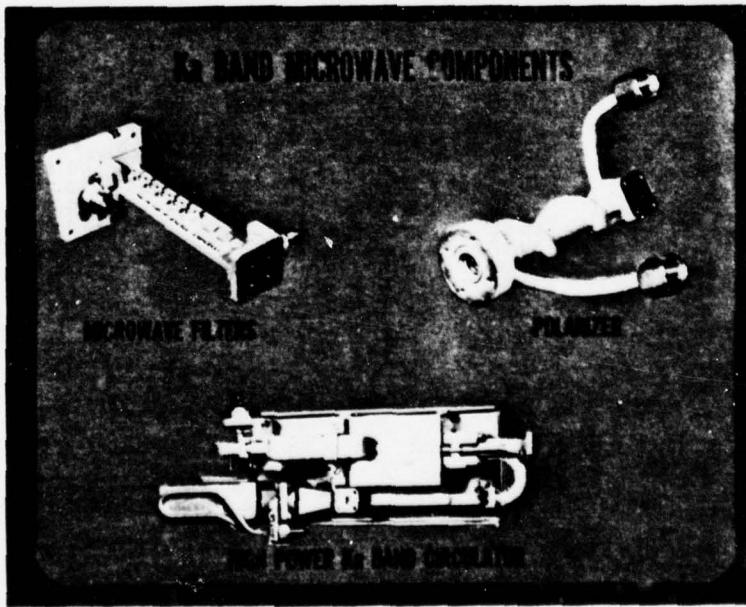
Figure 4-2. Ka Band Components in Rectangular Waveguide
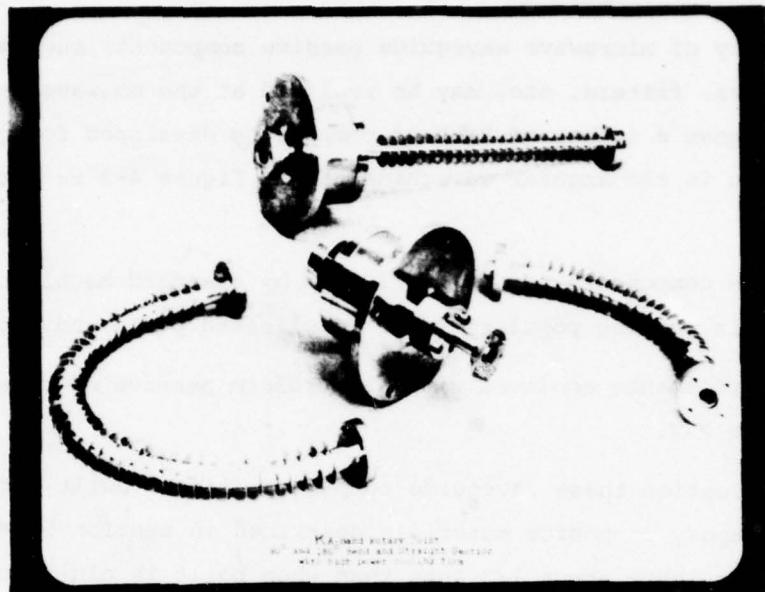
Figure 4-3. Ka Band Components in Circular Waveguide

Table XXV. Performance of Electroformed Passive Components

Component	Center Frequency (GHz)	Bandwidth	Insertion Loss (dB)	Isolation (dB)	VSWR
3 dB short slot	30-37	4 GHz	0.2	25	1.1
hybrid	55-63	8 GHz	0.5	20	1.2
Fixed tuned band-	30-38	400 MHz	0.2	—	1.1
pass filters	55-65	200 MHz	0.3	—	1.2
High pass	30-38	—	0.12	30*	1.2
filters	55-60	—	0.5	50*	1.25
Circulators	32-36	8 GHz	0.2**	20	1.1
	55-65	2 GHz	0.3	20	1.2
WG-coaxial transition	35	10 GHz	0.2	—	1.2
Passive power divider	37	6 GHz	0.2	20	1.2

*1.0 GHz Below Design Pass Frequency   **0.1 dB Over 5 GHz

4.2 MIC TECHNOLOGY[*]

Of the methods shown in Figure 4-1 the lowest-loss transmission lines are dielectric waveguide, conventional metal waveguide and dielectric-filled waveguide. Unfortunately, none of them can be considered planar, a distinct disadvantage over those that may be processed in volume using photolithographic techniques. Conductor loss of more convenient microstrip is about 0.2 dB/wavelength.

For each of fabrication and compatibility with semiconductor devices, those transmission lines that are particularly promising at millimeter wavelengths are:

- Coplanar waveguide
- Slotline
- Fin line
- Image line
- Microstrip
- Suspended stripline

A coplanar transmission line consists of a strip of thin-metallic film deposited on the surface of a dielectric substrate with two ground electrodes running adjacent and parallel to it on the same surface. The rf energy is confined to a closed area and the conducting elements permit easy connection of active devices in hybrid integrated circuits. It is ideal for shunt connection elements in monolithic MIC systems. Coplanar line has the advantage of having all the conducting elements on the same side of a dielectric substrate; standard MIC photolithographic and etching techniques are applicable. Coplanar line, enclosed in a channel, has been successfully used at frequencies to 60 GHz.

Slot transmission lines particularly useful for applications requiring regions of circularly polarized magnetic field and/or shunt-mounted elements. Slotline consists of two conductors separated by a gap on one side of a dielectric substrate.

---

*R. Davis "mm Wave Transmission Media" Microwaves, March 1976

Combined microstrip and slotline circuitry seem to offer possibilities with the advantage of easy coupling through the substrate from one medium to the other. Slotline is well understood and can be fabricated using standard MIC photolithographic and etching techniques. Such transmission line techniques, enclosed in a channel, have been successfully used for the design of tapered transformers to 60 GHz.

When slotline is used in a channel--that is, when the slotline substrate bridges the broad walls of a rectangular waveguide--it is sometimes called fin line. In effect, the line is a printed ridged waveguide and can be designed to have a wider useful bandwidth than conventional ridged waveguide. Integrated fin line can provide bandwidths in excess of an octave with less attenuation than microstrip. This adaptation of ridged-loaded waveguide permits circuit elements to be fabricated at low cost and is compatible with thin-film hybrid techniques. In passive circuits, such as filters, the fins may be directly grounded to the waveguide, and lumped elements, such as beam-lead capacitors, may be added. The gap between the fins can be varied along the longitudinal axis to provide low-cost circuit elements. When semiconductor devices are to be added, at least one of the fins must be dc isolated from ground to permit the application bias. In both approaches, the waveguide is parted along a plane where the current flow is parallel to the break, as in a common slotted line. During the past few years, fin line components have been fabricated successfully up to 40 GHz, and existing beam-lead devices in a simple fin-line mount may be useful beyond 80 GHz. However, it is expected that mechanical tolerance of the assembly may become important much above 60 GHz.

Low-loss propagation at millimeter wave, submillimeter wave and even optical frequencies is theoretically realizable using refractive dielectric guides and image guides. In theory, image guide is suitable for active integrated-circuit construction because the image plane can provide mechanical support to the dielectric material and also serve as heat sink and electrical ground to the integrated active devices. However, there are many practical fabrication and process problems that some researchers are trying to resolve at this point. In addition, metallic shielding around the image-guide is often necessary to reduce any radiation losses and eliminate any external electromagnetic interference.

4-10

Although rectangular dielectric guide has been applied at optical frequencies using low-dielectric constant materials, only recently has this type of guide been used at millimeter-wave frequencies using high-dielectric constant materials. The potential of rectangular dielectric guide millimeter-wave integrated circuits has been greatly enhanced using high-resistivity semiconductors such as silicon and GaAs as dielectric material.

Standard microstrip is one media where considerable effort had been spent. With this technique, Impatt oscillators have been developed at 30 GHz, 60 GHz and 100 GHz using quartz substrates at Bell Laboratories. Similarly, microstrip techniques have been applied to design 18-26 GHz balanced and image-rejection mixers and 18-26 GHz and 26-40 GHz polar discriminators using 0.010-inch thick sapphire substrates. Also, several researchers have used MIC techniques to fabricate broadband components up to 60 GHz using low dielectric substrates with dielectric constant of 2.5.

There are several difficulties that arise in extending microstrip over 60 GHz for low-loss circuits. These include critical tolerances, fragile substrates and radiation losses. The radiation losses can be eliminated by properly spacing the microstrip circuit in a channel. Some researchers have demonstrated the use of microstrip techniques up to a frequency of 100 GHz using fused silicon as the base substrate. The mechanical problems can be overcome with careful design techniques.

Suspended stripline is essentially the same as conventional stripline. However, the transmission line is inhomogeneous because of the presence of the dielectric. As a result, high-order modes can propagate. Also, the presence of any discontinuity can cause radiation losses and higher-order modes. These can be suppressed if the suspended stripline is enclosed in a rectangular guide. The dimension tolerances and surface finish on the metallic surroundings are not critical, as compared to a standard waveguide transmission line. Such transmission line techniques enclosed in a channel have successfully been used up to 60 GHz.

Regardless of the type of planar transmission media chosen, it appears that all the millimeter circuits require metallic shielding in order to control higher-order modes, reduce radiation losses and eliminate external electromagnetic

radiation interference. Generally, mode control becomes critical at higher frequencies and for broad bandwidth circuits.

In the selection of a particular transmission line, the following characteristics should be considered:

- Maximum achievable bandwidth
- Low loss or high unloaded Q
- Low-cost processing and fabrication techniques
- Ease in bonding or attaching active components
- Radiation losses
- Susceptibility to external electromagnetic interference.

4-12

SECTION 5

ANTENNA SUBSYSTEMS

For the mm Wave Satellite communication bands considered, reflector, lens antennas and phase arrays have been used or studied for different applications.

Table XXVI summarizes the present state of the art and future projections for the application of these technologies to antennas to be used in ground terminal and space applications.

5.1 GROUND ANTENNAS

As shown in Table XXVI, for mm Wave satellite communication ground terminals, reflector antennas, lens antennas and phase arrays are suitable candidates. Each of these technologies has its own area of application, but still the reflector type of antenna provides the best performance and cost, and will be of preponderant use. Lens and phase arrays may find their use for small antennas and for mobile platforms.

5.1.1 REFLECTOR ANTENNAS

The design considerations for a ground terminal reflector antenna are:

- Antenna gain and required reflector size
- Allowable rms surface tolerance deviation
- Pointing and tracking accuracy
- Antenna noise temperature
- Aperture illumination (feed design)
- Sidelobe levels
- Cost

At mm wave the achievable gain may be limited by the surface tolerance achievable for a given reflector size as expressed by Ruze's formula:

Table XXVI. Antenna Technology for mm Wave Satellite Communications

APPLICATION	TYPE OF ANTENNA	TECHNOLOGY AVAILABILITY	
		CURRENT	10-15 YEARS
GROUND TERMINALS	REFLECTOR	X	X
	REFLECTOR MBA	STUDY AND FEASIBILITY	X
	LENS	PROTOTYPE	X
	PHASE ARRAYS	—	X
SPACE	REFLECTOR	X	X
	REFLECTOR MBA	STUDY AND FEASIBILITY	X
	LENS	STUDY AND FEASIBILITY	X
	PHASE ARRAY	—	?
	HORN	X	X

$$G = \eta \left(\frac{\pi D}{\lambda} \right)^2 \quad \exp - \left(\frac{4\pi\epsilon}{\lambda} \right)^2$$

where   G = gain of the antenna

D = reflector diameter

λ = free space wavelength

ϵ = rms surface tolerance deviation

η = radiating aperture efficiency

In general, the gain of an antenna having a fixed surface tolerance, first increases as the square of the frequency until the exponential terms takes over and a further increase in frequency results in a decrease in gain. The point at which the gain is maximized is called the gain limit point. Conversely for a given frequency the maximum useful aperture size will be limited by the achievable surface rms tolerance, since as the antenna aperture becomes larger, it is increasingly more difficult to provide a reflector with the required surface tolerance.

The surface tolerance of an antenna consist of the following factors:

a)   Aggregate reflector panel surface tolerance

b)   Reflector surface alignment (setting) tolerance

c)   Reflector backstructure gravity deflections

d)   Subreflector surface tolerance

e)   Reflector surface deviations due to wind loading

f)   Reflector surface thermal distortion

The last two items apply to exposed antennas only and will be neglible when the antenna is enclosed in a radome.

The state-of-the-art in the design and fabrication of large reflectors, where the rms tolerance will be the limiting factor, have considerably improved in particular for radio astronomy applications into the mm Wave region. Figure 5-1 shows the performance achieved with recent radiotelescope designs, useful for the bands considered in this study[*], and Table XXVII gives the characteristics of these antennas. Photographs of the 30 ft antenna in the test range and the radome

---

[*] Data from Electronic Space Systems Corp, Concord, Mass.

Wavelength (mm)

$$G = K_1 \cdot K_2 \cdot K_3 \cdot \frac{4\pi \cdot A}{\lambda^2} \quad G\ (dB) = 10\ Log\ G$$

A = Reflector Area, λ = Wave Length

K_1* = 0.65 Nominal. Includes Feed Taper,
Spillover. Total Aperture Blockage
(Radome. Subreflector. Supports) etc

K_2 = Radome Membrane Factor
Curves Plotted with K_2 = 1

K_3* = Reflector Tolerance
(rms Error) Factor

A280
A260
A220
A230
A240

*For exposed Reflectors
K_1 & K_3 may be
seriously degraded by
the overall environment

Reflector Gain dB (G)

Frequency(GHz)

Figure 5-1.   Performance of Current Radiotelescope Antennas

Table XXVII.   Characteristics of Radiotelescope Antennas

	A220	A230	A240	A260	A280
Reflector Aperture	23 ft (7.0 m)	33 ft (10.0 m)	45 ft (13.7 m)	66 ft (20.1 m)	88 ft (26.8 m)
F/D	0.45	0.31	0.37	0.45	0.34
Subreflector Diameter	24 in (61 cm)	35 in (89 cm)	43 in (108 cm)	66 in (168 cm)	92 in (234 cm)
Radome Diameter	41 ft (12.5 m)	48 ft (14.6 m)	68 ft (20.7 m)	100 ft (30.5 m)	132 ft (40.2 m)
Reflector Surface Tolerance at Elevation angles between 30° and 90°	0.1 mm rms	0.12 mm rms	0.13 mm rms	0.15 mm rms	0.17 mm rms
Pointing/Tracking Accuracy	0.001 degrees				
Velocity Range	0.001 to 1 degree/second				
Acceleration	1 degree/second²				
Positioning Precision (Computer Controlled)	Full Parallel 22 Bit Binary Plus Sign				

enclosed 66 ft are shown in Figures 5-2 and 5-3. Figure 5-4 shows what is believed to be the limit currently achievable for large reflectors surface tolerances for radome enclosed and exposed antennas to the environment (no MIL spec) that may be found in normal mid latitude fixed sites, with no ice or snow accummulation on the surfaces.

Using this data the estimated recurrent cost (not including feed) for antennas optimized at the 20/30 GHz band are shown in Figure 5-5, and for the 40.5/43-45 GHz band in Figure 5-6.

It is apparent that very large antenna gains are now feasible at these frequencies and the accurate pointing with or without autotrack becomes a consideration for the larger apertures. The pointing inaccuracies of an exposed antenna result from many sources as listed in Table XXVIII. Items 2, 3, 4 and 5 may be eliminated by enclosing the antenna under a radome, but this will introduce a boresight shift, which can be designed to be very small. For a receiving antenna, autotracking will eliminate this later effect, as well as gravity deflection errors, the effects of steady wind, thermal differentials, deflections due to ice loading of the structure, and readouts and site surveying errors.

The above considerations mainly apply to a Cassegrain reflector geometry, however, other geometries such as spherical and torus have been considered in particular for multiple beam antennas, where a ground terminal is to operate with more than one satellite.

Figure 5-7 shows a prototype torus reflector antenna suitable for operation in the 20/30 GHz band and at higher frequencies[*]. This antenna consists of a 30 ft torus main reflector and a shaped subreflector shown in Figure 5-8 given a 20° field of view and the gain characteristics shown in Figure 5-9. Limited antenna pointing is done by moving the feed, with the resultant cost economy. Also, the difraction effects of the subreflector are eliminated resulting in the sidelobes reduction required for close orbit spacing of multiple satellites.

_____

* R. Kreutel "A Multiple Beam Torus Reflector Antenna" AIAA/CASI 6th Communications
 Satellite Systems Conference, Montreal, 1976
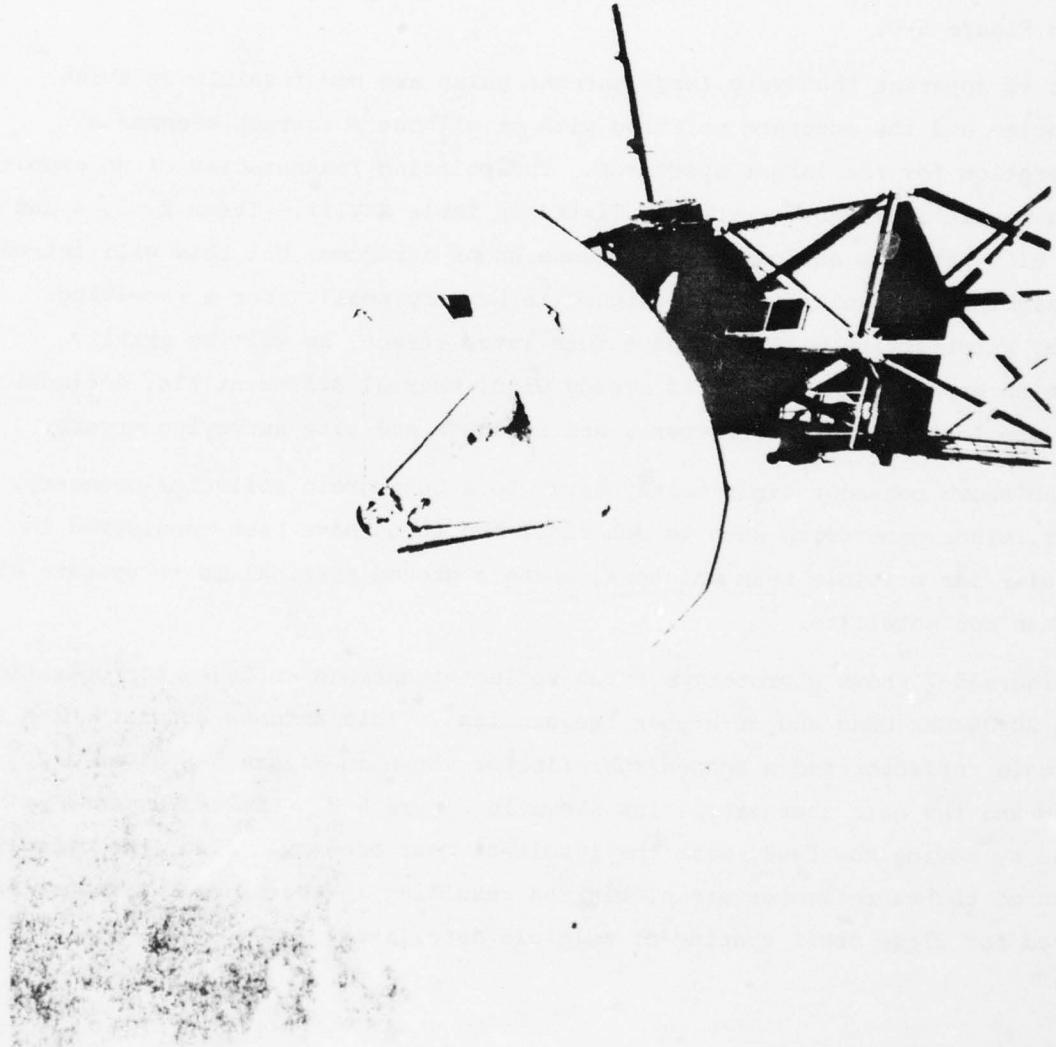
Figure 5-2. 30-foot Diameter Reflector Undergoing Pattern Test at the ESSCO Antenna Range, Concord Mass.
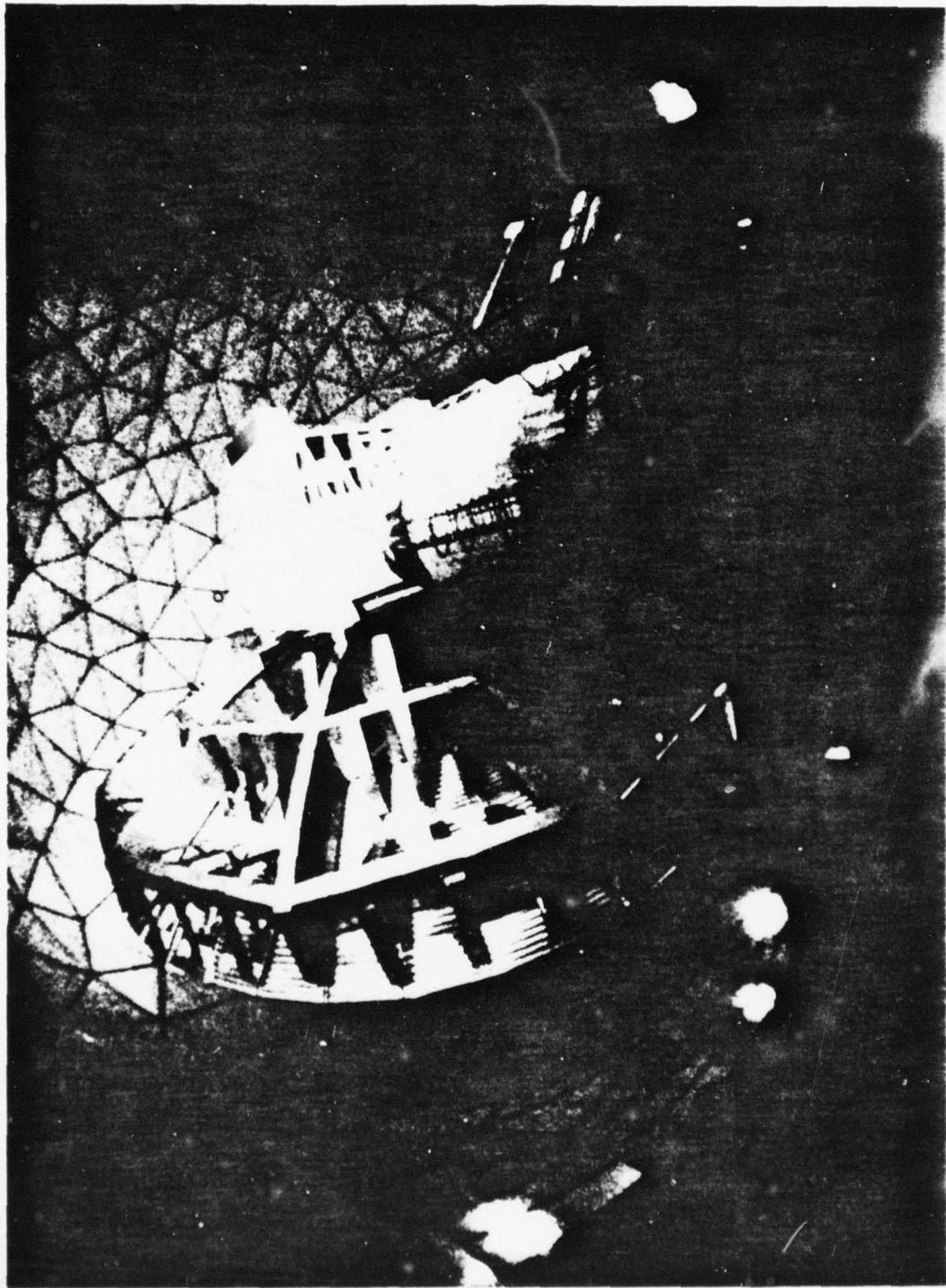
Figure 5-3. Interior View of Completed 60 ft Radiotelescope Antenna System
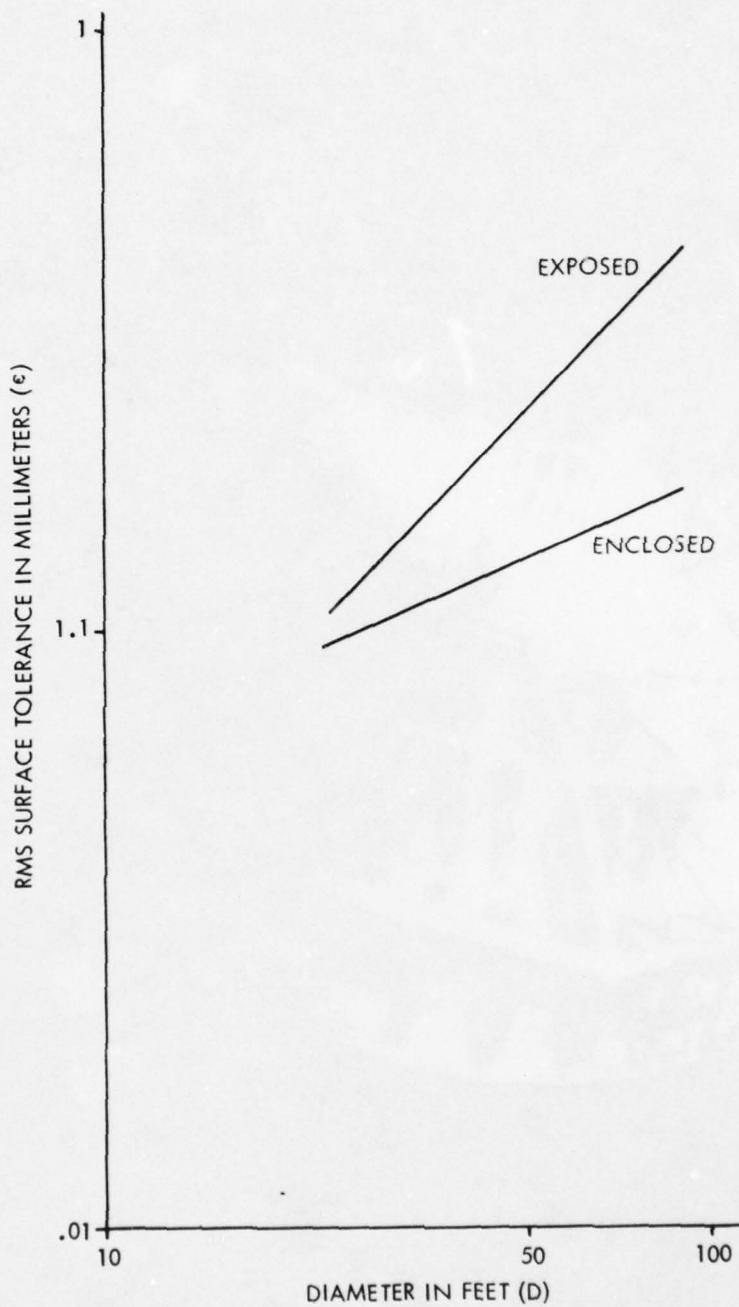
Figure 5-4. RMS Surface Tolerance in Millimeters (ϵ) of "State-of-the-Art" Large Reflector Antennas
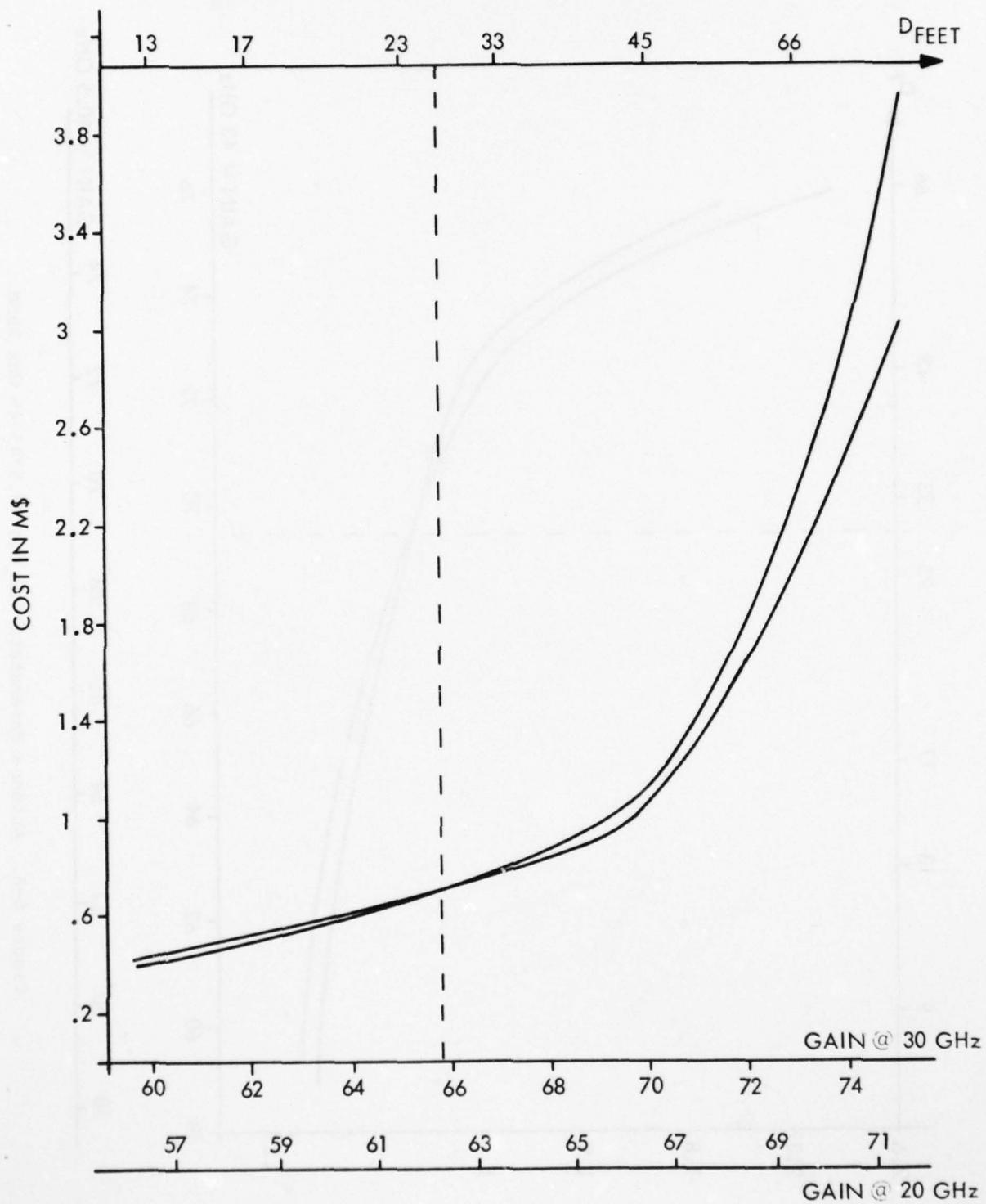
Figure 5-5. Antenna Parameters for 20/30 GHz Band

Figure 5-6. Antenna Parameters for the 40.5/43-45 GHz Band
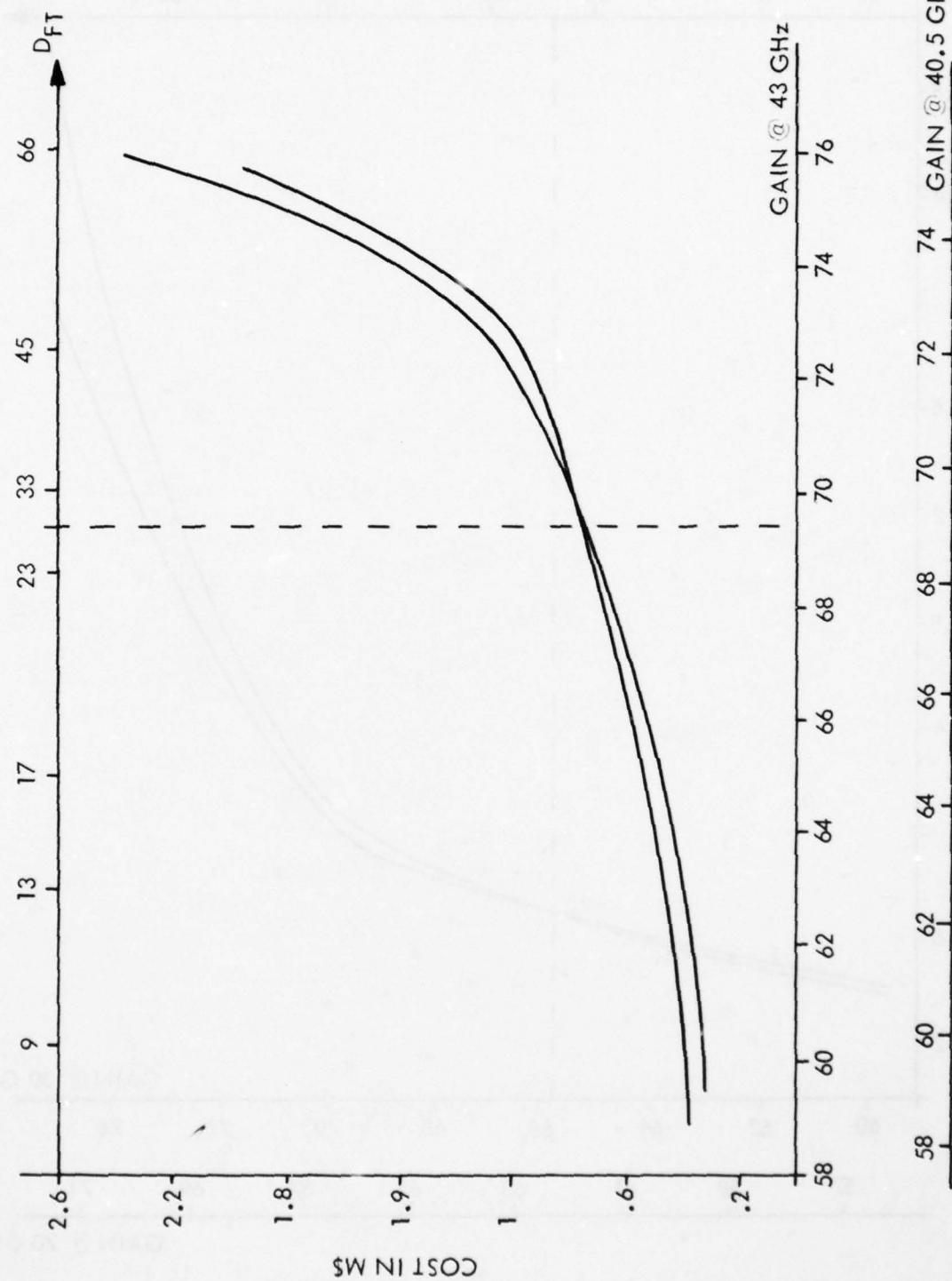
Table XXVIII. Pointing Accuracy Error Sources

|	Components Affected			
Pointing Accuracy Error Sources	Reflector Assembly	Mount Assembly	Readout System	Servo System
1. Gravity - Deflections due to gravity lead variation with pointing angle.	X	-	-	-
2. Steady State Wind - Deflection due to constant velocity wind on structure.	X	X	-	-
3. Gusty Wind - Dynamic wind errors.	X	X	-	X
4. Thermal Differentials - Deflection of structure due to steady state temperature differentials.	X	X	-	-
5. Ice Loading - Deflection of structure variations with pointing angle.	X	-	-	-
6. Inertia - Deflection due to acceleration (negligible).	-	-	-	-
7. Manufacturing and Alignment Tolerances - Errors due to components, tolerances, orthogonality and alignments.	X	X	X	-
8. Tracking Error - Servo Loop Error.	-	-	-	X
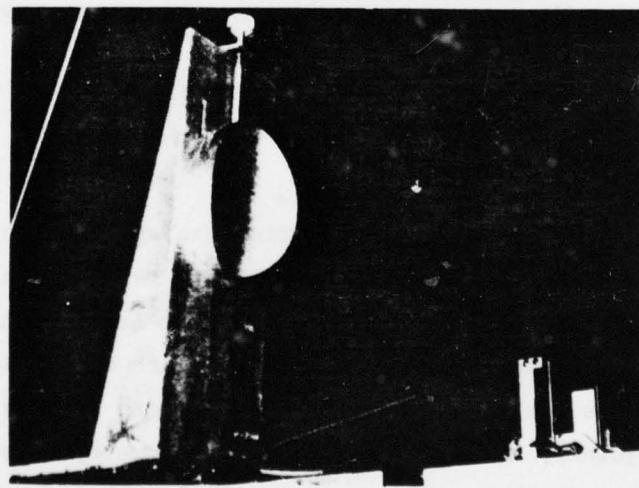
Figure 5-7. Feed System of Phased-Connected Torus Antenna

Figure 5-8. Experimental Model of the Phase Connected Torus Antenna
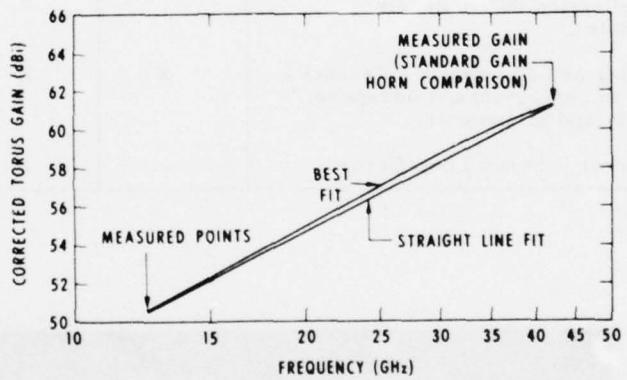
Figure 5-9. Measure Gain vs Frequency for the Corrected Torus

5.1.2 LENS ANTENNAS

Lens antennas for ground terminals may find its application for small aperture sizes, as illustrated by a Lunenberg lens capable of being installed at the top of a submarine periscope. The advantage of a dielectric lens antenna vs a conventional reflector antenna is that the thick radome is made part of the lens system, that the antenna feed remains stationary while the solid lens rotates eliminating the necessity of rotary joints, and that the resultant geometry is very compact and capable of installation in the small volume available.

5-12

This concept, as shown in Figure 5-10, consists of a modified hemispherical quartz Lunenberg lens with a metallic reflection, mounted in a two axis gimball (elevation over traverse), inside a 270° quartz spherical radome with an embedded circular waveguide horn/feed.

The two section lens consists of an outer quartz sphere an inner ball with slightly higher dielectric consistent resulting in the following estimated performance:

Gain @ 0° scan	33.8	dB
Gain @ 65° scan	32.8	
1st Sidelobe @ 0° scan	-24	dB
1st Sidelobe @ 65° scan	-22	dB
Far out sidelobes @ 0° scan	-48	dB
Far out sidelobes @ 65° scan	-45	dB
VSWR	1.15:1	
Axial ratio	1	dB

5.1.3 PHASE ARRAYS

Phase array antennas for mm Waves satellite communication or even at SHF, have not been used in part due to cost, complexity and lower G/T for a given aperture size. There are, however, two areas where phase arrays may find an application in the future: in conformal arrays for high performance aircraft and to form multiple beams, giving the possibility to operate with more than one satellite at a time.

At SHF, one approach investigated for phase array satellite communication antennas consist of distributed transmit and receive modules as shown in Figure 5-11 arranged in a conformal array surface in the configuration of Figure 5-12 to provide hemispherical scannable coverage of the radiated or receive pattern above the aircraft.
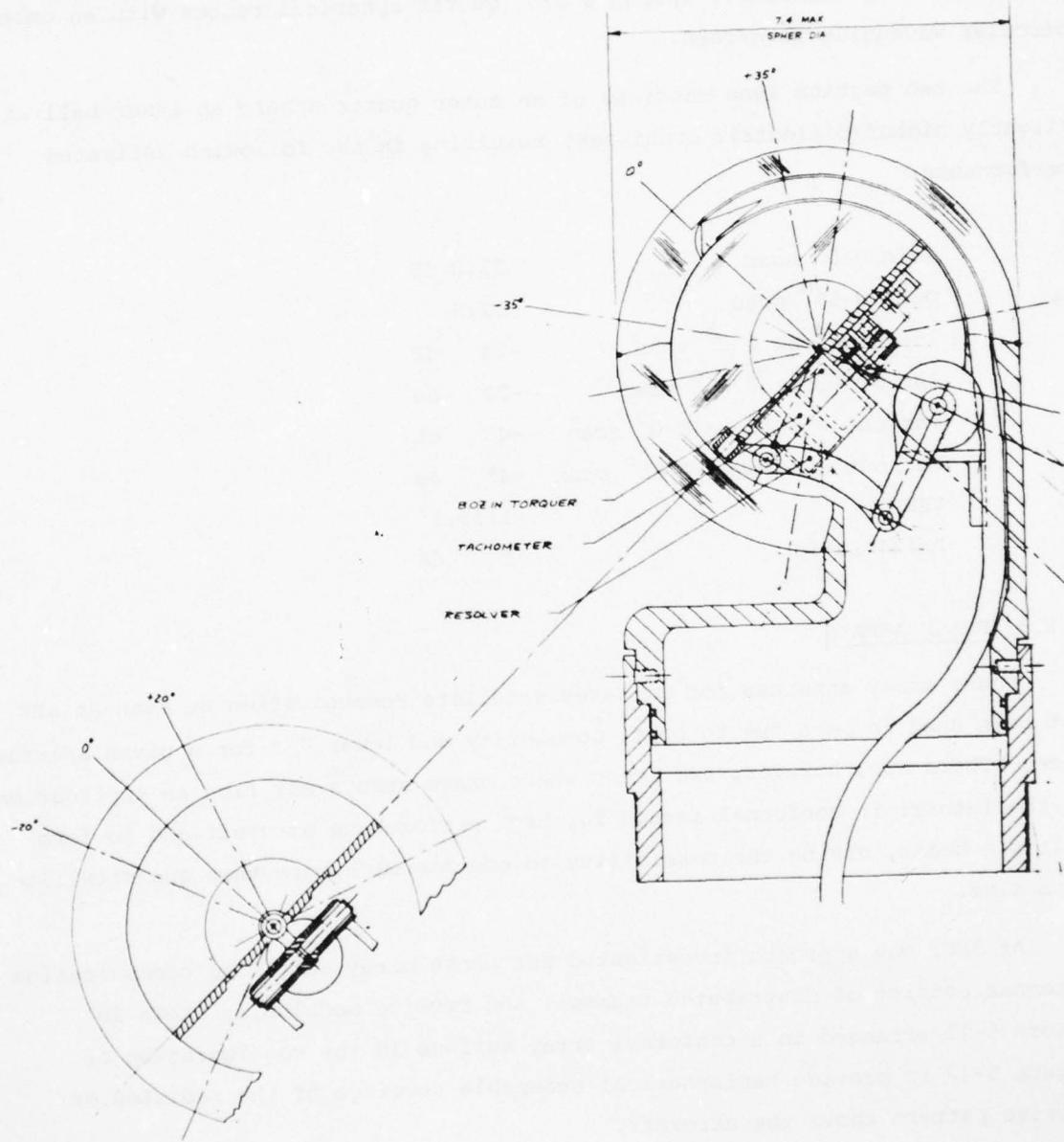
Figure 5-10. Lens Antenna
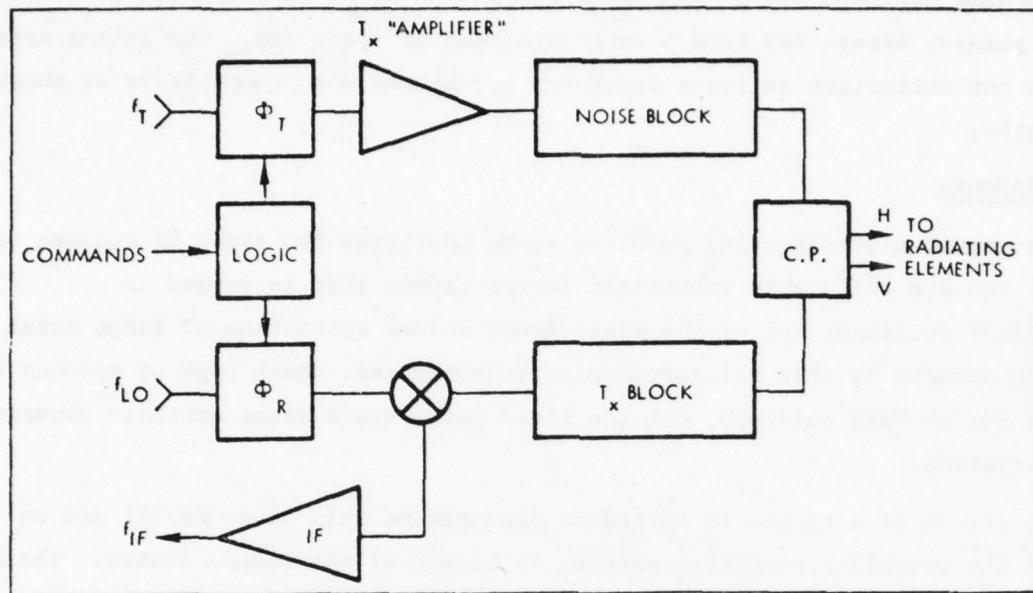
Figure 5-11.   Functional Block Diagram of Module
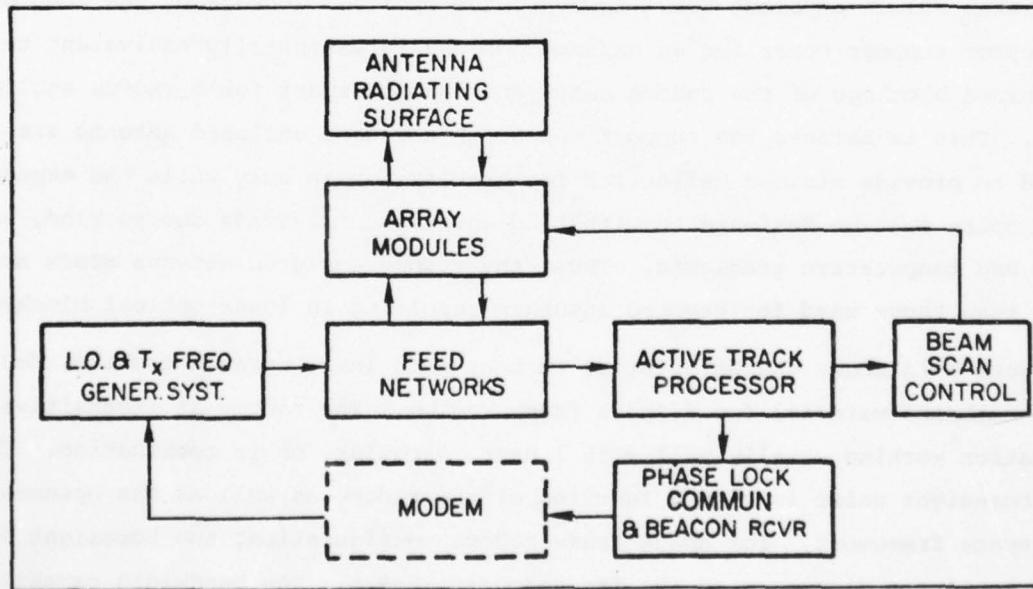
Figure 5-12.   Major Hardware Elements of Airborne Terminal Using
a Phase Array Antenna

The same approach may be conceivable implemented at EHF, as well as others such as passive arrays fed from a corporate feed or space fed. The latter approach which is not attractive at lower frequency may become more competitive at shorter wavelengths.

5.1.4 RADOMES

For ground stations using relative large apertures two types of radomes used are: a) the air inflatable rubberized fabric radome that is seemed in longitudinal sections; and b) the metal frame radome consisting of large metal framework covered by thin reinforced plastic membranes. Both type of radomes are suitable for mm Wave antennas, but the rigid metal space frame exhibits superior characteristics.

The effect of a radome is to reduce the antenna gain given by (1) and to increase the overall system temperature, as result of the radome losses. The latter, for a space frame rigid radome, result from aperture blockage caused by the metal frame plus membrane dielectric path losses. The aperture blockage result in a reduction of the antenna efficiency, where for mm wave radiotelescopes result in experimental values of about 65%. However, the optical blockage of the feed or subreflector support spars for an exposed antenna is essentially equivalent to the combined blockage of the radome beams and support spars for a radome enclosed antenna. This is because the support spars for a radome enclosed antenna are designed to provide minimum deflection for gravity forces only while the exposed antenna spars must be designed to withstand environmental loads due to wind, snow and ice and temperature gradients. Thus, the radome enclosed antenna spars are lighter than those used for exposed antennas resulting in lower optical blockage.

Figure 5-13 shows characteristics such as path loss, boresight shift, for a typical membrane material for a space frame radome. The radome is insensitive to polarization working equally well with linear, circular, or in combination. The radome boresight shift is also a function of the radome as well as the openness of the space framework. For space frame radome configuration, the boresight shift is very small and decreases as the frequency increases. The bandwidth capability is extremely broad as evidenced in Figure 5-13.

Figure 5-13. Typical Electrical Performance Radome Enclosed Antenna
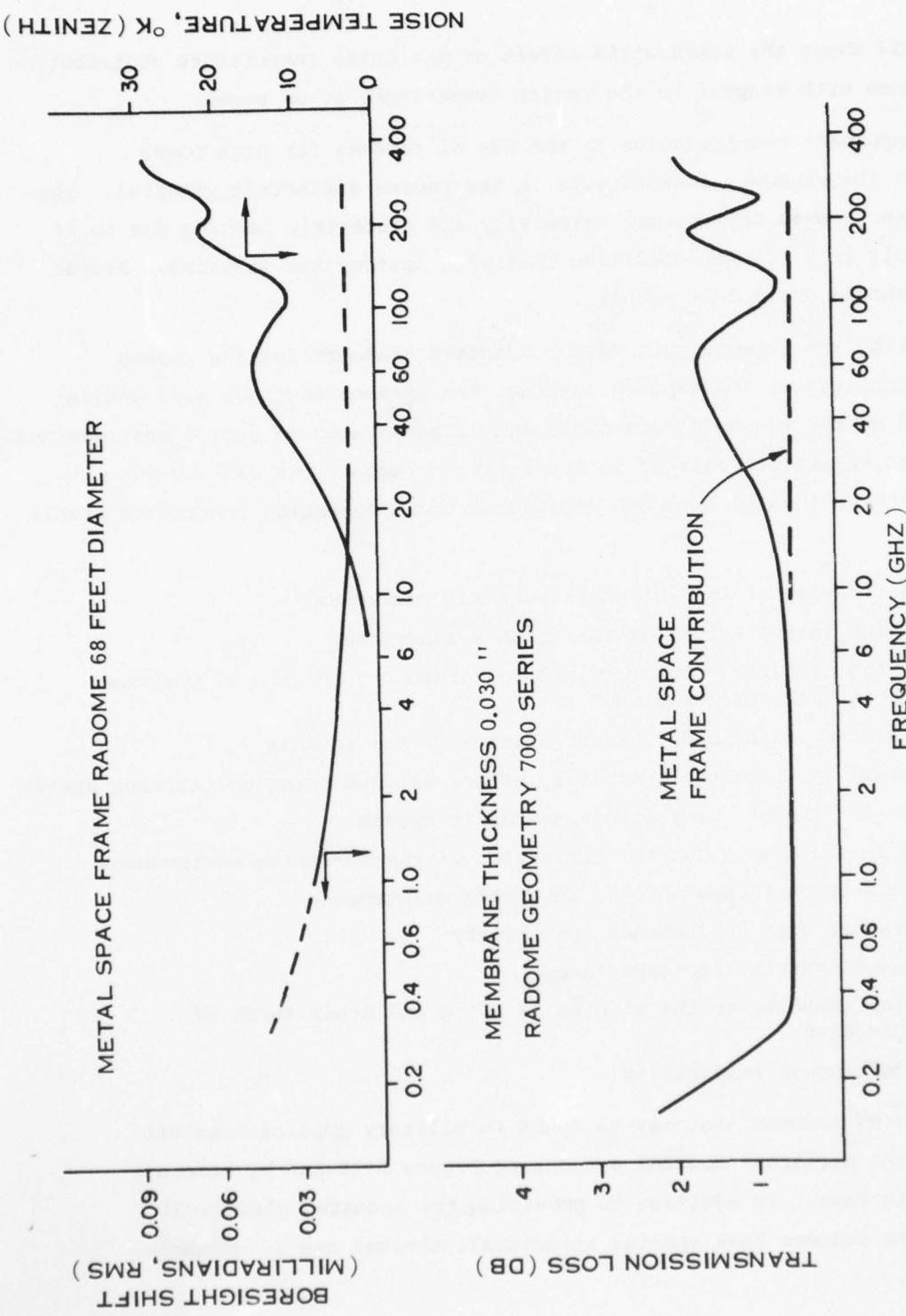
NOTE—
ABOVE VALUES ARE BASED ON MEMBRANE LOSS CALCULATIONS, MODEL METAL SPACE FRAME MEASURMENTS, AND OBSERVED FULL SCALE DATA. ACTUAL VALUES VARY SLIGHTLY AS THEY ARE DEPENDENT ON ANTENNA SIZE, TYPE AND LOCATION IN THE RADOME.

Figure 5-14 shows the comparative effect of the noise temperature contribution due to the radome with respect to the zenith temperature at mm waves.

Another important consideration in the use of radomes for high power application, is the rf power loss effects in the radome dielectric material. The improper balance between the thermal emissivity and dielectric heating due to rf losses may result in a runaway condition that will destroy the material. Proper radome design should avoid this problem.

In conducting the antenna gain versus diameter tradeoff for the radome sheltered antenna against the exposed antenna, the systems engineer must obtain an appreciation of the radome's advantages and disadvantages to derive cost savings. In balancing the additional cost of incorporating a radome, one can perceive the apparent cost savings of a radome enclosed antenna operating controlled stable environment:

a.   Simplification of the antenna structural subsystem

b.   Reduction in the weight of the antenna subsystem

c.   Reduction of drive power required to rotate the antenna at various velocities and accelerations

d.   More uniform rotational characteristics of the antenna

e.   Increased and repeatable accuracy of the antenna pointing tracking system

f.   Increased life of the bearings and drive system

g.   Reduced maintenance due to elimination of the corrosive environment

h.   More easily performed antenna subsystem maintenance

i.   All weather high performance operability

j.   Increased overall life expectancy

k.   Inherent immunity to the effects of icing and other forms of precipitation

l.   High continuous reliability.

Other types of radomes that may be found in military applications are exemplified by the periscope mounted antenna of Figure 5-10 and by aircraft radomes. In both cases, in addition to providing the required electrical performance these radomes have special structural, thermal and aerodynamic characteristics.

1·0 2·8 2·5

5·0 3·15 2·2
5·6 3·5

1·1 4·0 2·0
4·5

1·8

1·25 1·4 1·6

NATIONAL BUREAU OF STANDARDS
MICROCOPY RESOLUTION TEST CHART

NOISE TEMPERATURE, °K

H_2O

H_2O

O_2

O_2

H_2O

FREQUENCY, GHz

ATMOSPHERIC NOISE TEMPERATURE
AT ZENITH LOOK — LOW
WATER VAPOR CONTENT

NOISE TEMPERATURE CONTRIBUTION
OF RADOME MEMBRANE
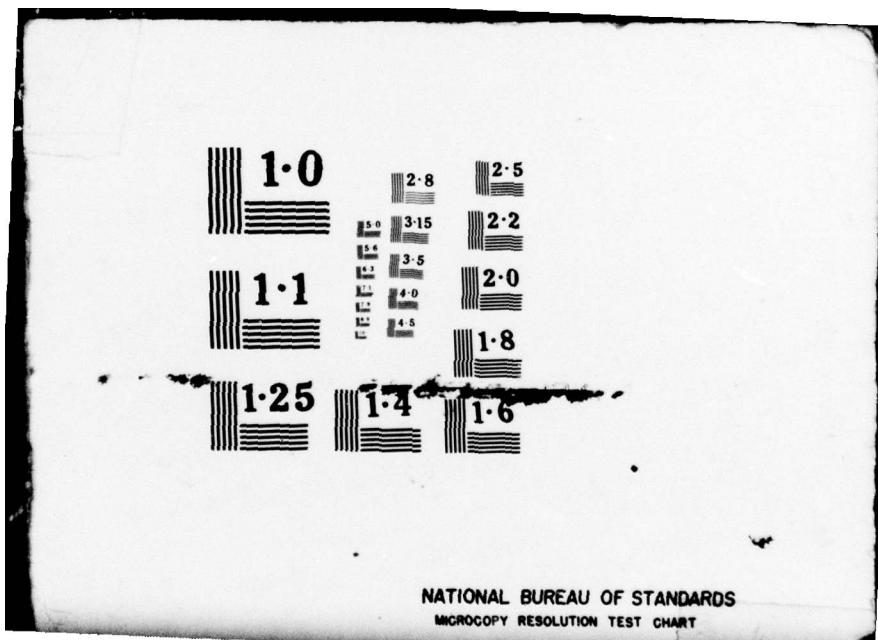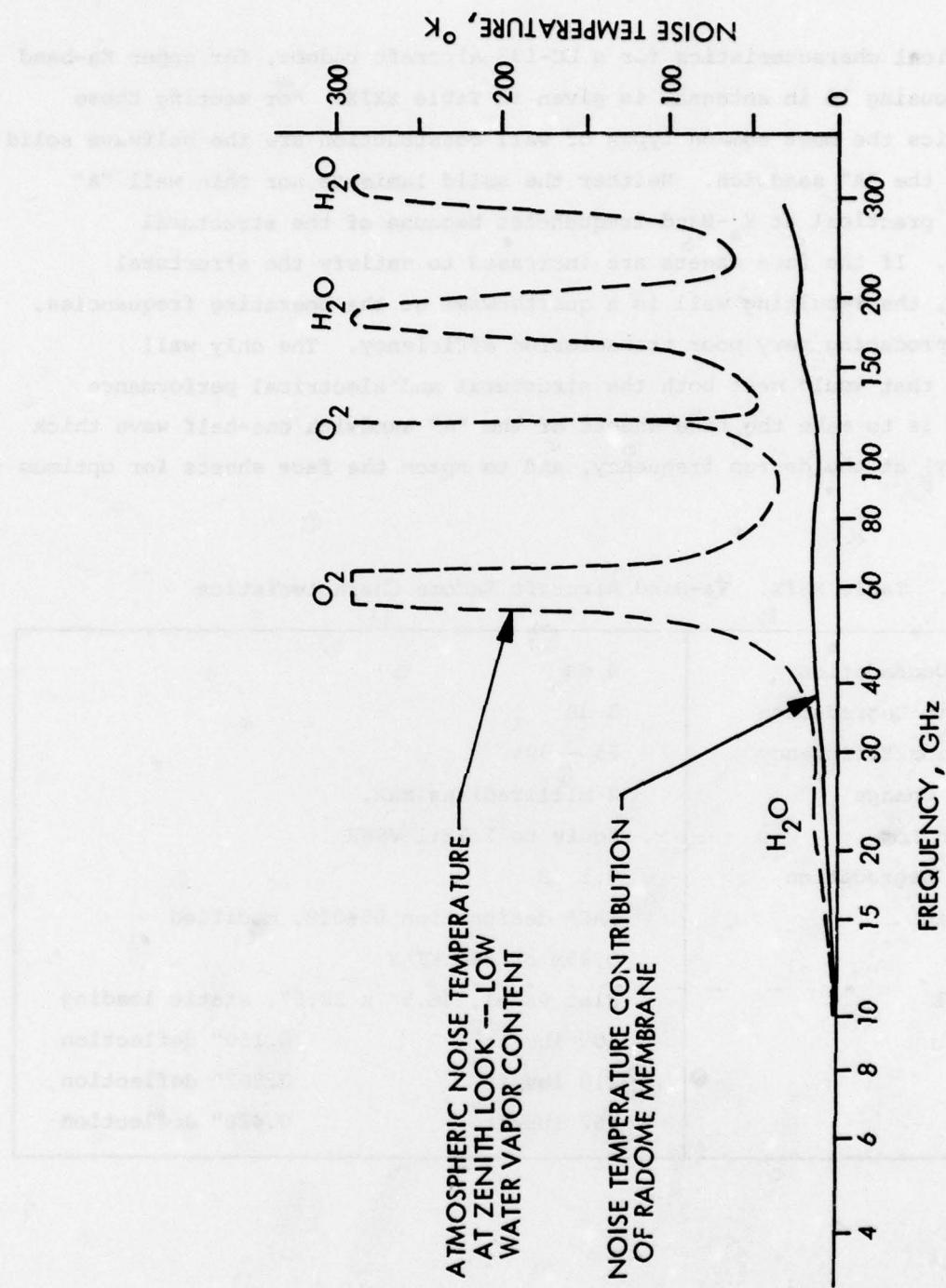
Figure 5-14. Atmospheric and Radome Noise Temperature

5-19

The typical characteristics for a EC-135 aircraft radome, for upper Ka-band capable of housing 36 in antenna, is given in Table XXIX. For meeting these characteristics the most common types of wall construction are the halfwave solid laminate and the "A" sandwich. Neither the solid laminate nor thin wall "A" sandwich are practical at K_a-Band frequencies because of the structural requirements. If the face sheets are increased to satisfy the structural requirements, the resulting wall is a quarterwave at the operating frequencies, a condition producing very poor transmission efficiency. The only wall construction that would meet both the structural and electrical performance requirements is to make the face sheets of the "A" sandwich one-half wave thick (electrically) at the design frequency, and to space the face sheets for optimum performance.

Table XXIX. Ka-Band Aircraft Radome Characteristics

Sidelobe Degradation	4 dB
Axial Ratio Degradation	3 dB
Transmission Efficiency	75 - 90%
Boresight Change	2 milliradians max.
Reflection Loss	Equiv to 1.22:1 VSWR
Crossover Degradation	0.1 dB
Aerodynamic	NACA designation 65-018, modified
Airspeed	0.95M or 394 KIAS
Structural	Flat Panel, 46.5" x 22.5", static loading
	109 lbs/ft^2 0.150" deflection
	218 lbs/ft^2 0.267" deflection
	462 lbs/ft^2 0.428" deflection

In this type of construction, shown in Figure 5-15, two face sheets are separated by a honeycomb structure. The face sheets are made of a high temperature polyester with "E" glass, i.e., UPS P-680 prepreg. The prepreg is perferred in order to control the resin to glass ratio so a uniform dielectric constant is obtained. The thickness of the face sheets was determined by the electrical requirement on high transmission efficiency and the thickness of the honeycomb was calculated to meet the structural strength experiment. Because the finished radome was to have a thin anti-static coating over much of the exterior surface and a thin rain-erosion coating over the nose area, the thickness of the outside face sheet is 0.005 inches thinner than the inside face sheet as illustrated in the Figure 5-15. The coating materials used are polyurethane for rain-erosion and an epoxy for anti-static characteristics.
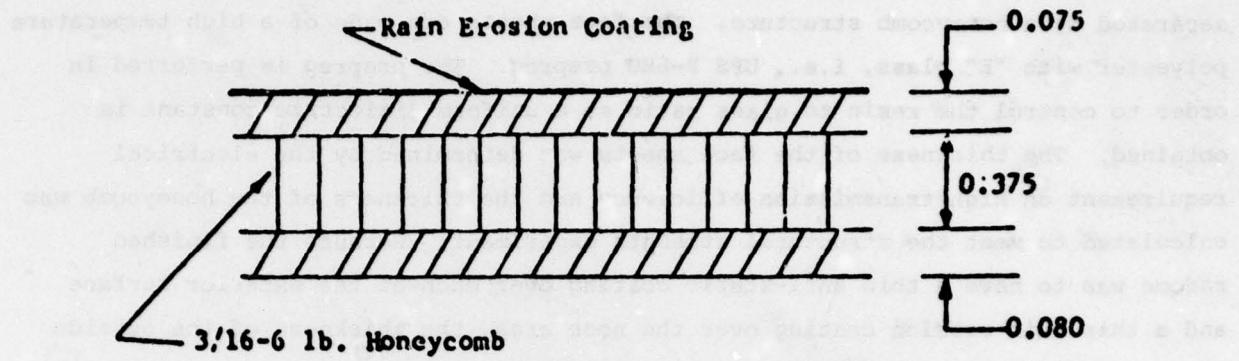
Figure 5-15. mm Wave Aircraft Radome Skin Construction

5.2 SPACECRAFT ANTENNAS

Horns, cassegrain and offset feed reflector and lens will find, application
for mm wave spacecraft antennas. The use of phase arrays seem questionable at this
time, in favor of MBA for providing the same type of performance.

5.2.1 REFLECTOR TYPE OF ANTENNAS

High gain spacecraft reflector type mm wave antennas may be built of light
metals such as alluminum, titanium and invar, or of composite materials. The use
of large gain antennas at mm wave frequencies in the space environment will impose
additional problems of thermal stability, high rigidity and tight tolerances, at the
same time that maintaining a light structure. The newly developed composite
materials show a dramatic figure of merit (defined as relationships of stiffness
divided by density and thermal expansion coefficient) in comparison to the other
metals, and will probably be preferred in future spacecraft antenna construction.
Figure 5-16* projects the antenna gains achievable with this type of construction,
both for fixed reflectors contained within the payload envelope of a standard
spacecraft and the Shuttle Interim Upper Stage, and for erectable antennas.

---

*T. Fager "Application of Graphite Composites to Future Spacecraft Antennas"
AIAA/CASI 6th Communication Satellite Systems Conference, Montreal, 1976.
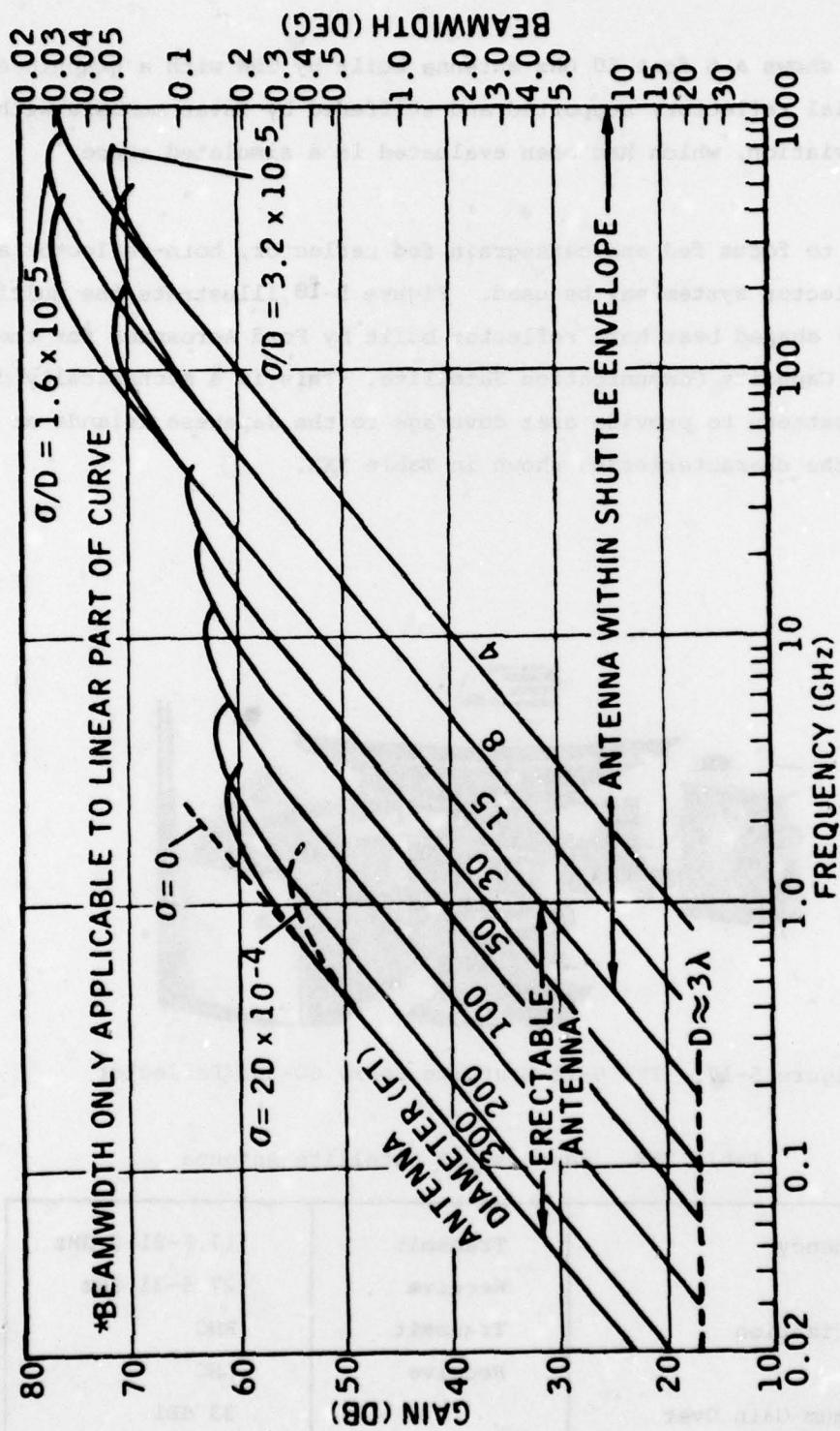
Figure 5-16. Projected Gain of Graphite Antenna System

Figure 5-17 shows a 6 foot 60 GHz antenna built by TRW with a graphic-epoxy composite material reflector, supported and stiffened by Invar members with a 0.001 in rms deviation, which has been evaluated in a simulated space environment.

In addition to focus fed and cassegrain fed reflector, horn-reflector and offset feed reflector system may be used. Figure 5-18 illustrate the multiband (4/6; 20/30 GHz) shaped beam horn reflector built by Ford Aerospace for the Japanese Medium Capacity Communication Satellite. This is a mechanically de-spun antenna with a pattern to provide area coverage to the Japanese Islands at 20/30 GHz and having the characteristics shown in Table XXX.
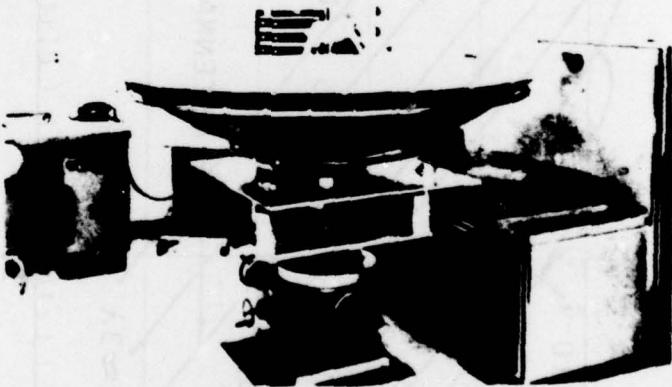

Figure 5-17. TRW 6-ft Graphite Epoxy 60-GHz Reflector

Table XXX. Japanese CS Satellite Antenna

| Frequency | Transmit | 17.7-21.2 GHz |
	Receive	27.5-31 GHz
Polarization	Transmit	RHC
	Receive	LHC
Minimum Gain Over Coverage Area		33 dBi
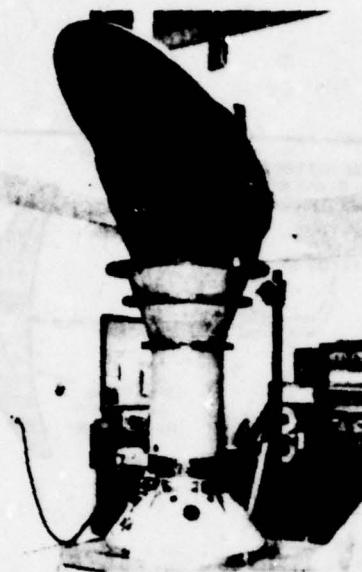
Figure 5-18. Multiband Shaped Beam Horn

Multiple beams may be also generated from reflector antennas,* as illustrated by a proposed spherical reflector multibeam antenna for the 20/30 GHz band shown in Figure 5-19. A labroatory model with a 150 cm diameter spherical reflector fabricated of urethane foam and epoxy materials and having 0.05 mm rms accuracy give the performance shown in Figure 5-20. The measured beam coupling is less than -35 dB, with half power beamwidth of 0.65° at both 19 and 30 GHz.

A similar arrangement of periscope type of antenna is being used in the LES 8/9 spacecraft, upper Ka-band (36-38 GHz) antenna, shown and used for either up/down link communication or for a crosslink between satellites. This antenna shown in Figure 5-21 in the crosslink orientation consist of an 18 in. diameter paraboloidal disk and feed system which illuminates the movable flat reflector which aims the beam. The beam moves up to 104° total in the orbit plane (E-W) about the pitch or Z axis and $\pm10^{\circ}$ out of the orbit plane (N-S) about an orthogonal axis in the roll/yaw (x/y) plane. The same picture also shows the Ka-band horn for area coverage. (9.5°). The characteristics of the antennas are given in Table XXXI. A tracking capability is incorporated to acquire and track the other satellite in the crosslink position by using sequential lobing of the five horn feed.

---

*R.H. Turrin "Multibeam Spherical Reflector Satellite Antenna for the 20/30 GHz Band" BSTJ July/August 1975.
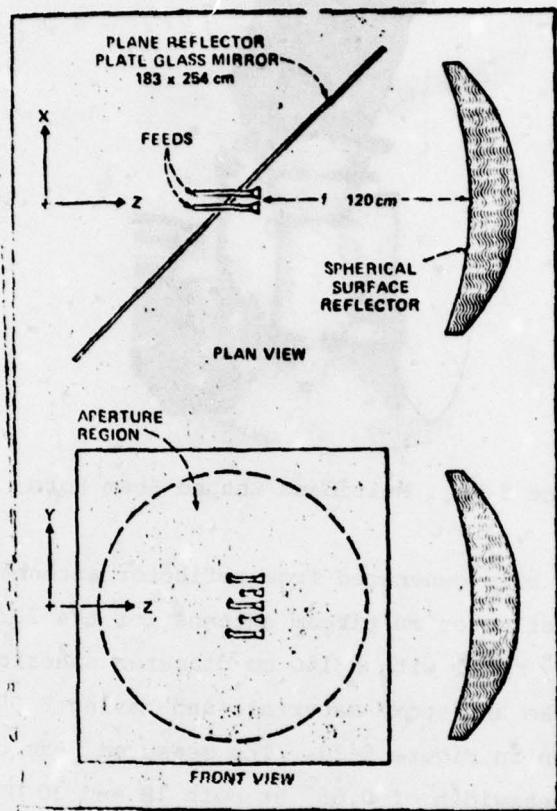
Figure 5-19. Spherical Reflector Multibeam Antenna
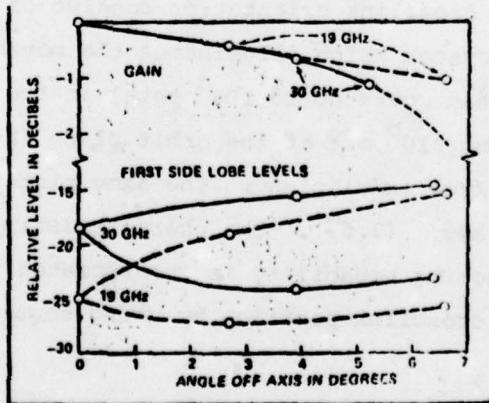
Figure 5-20. Single Feed Off-Axis Performance of Spherical Reflector
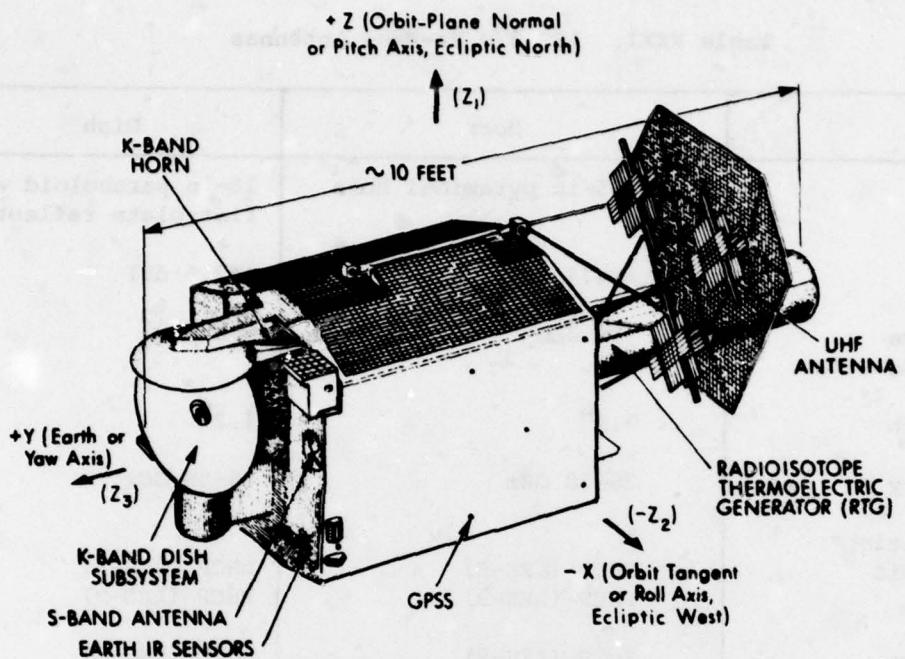
Figure 5-21. LES-9 Spacecraft Antennas

5.2.2 HORNS

mm Wave horns may be expected to find their application as earth coverage or area coverage antennas, and as feeds for the larger reflector type of antennas. Here again the construction may be in the future made of composite materials, as illustrated by the W-band antenna of Figure 5-22.

5.2.3 LENS ANTENNAS

Lens antennas may be design at mm wave for implementing electronic scanning multibeam operation of the spacecraft antenna.

Figure 5-23 illustrates the concept for a dual lens, array feed, at Q-band to provide stepping beam scanning of the field of view. This antenna uses two dielectric lenses providing two Fourier transforms to produce a magnified image of a small feed array in the aperture plane.

Table XXXI. LES 8/9 Ka-Band Antennas

|	Horn	Dish
Type	2.5-in pyramidal horn	18-in paraboloid with flat-plate reflector
Gain	+24.4 dBI	+42.6 dBI
Effective Receiving Area	-28 dBm^2	-10 dBm^2
Beamwidth	9.5°	1.2°
Frequency	36-38 GHz	36-38 GHz
Polarization* Transmit	LHCP (LES-8) RHCP (LES-9)	LHCP (LES-8) RHCP (LES-9)
Receive	RHCP (LES-8) LHCP (LES-9)	RHCP (LES-8) LHCP (LES-9)
Beam-steering (for nominal satellite attitude)	Fixed, squinted for particular footprints on Earth	104° in orbit plane** ±10° out of orbit plane***
Angle-tracking	None	Sequential lobing
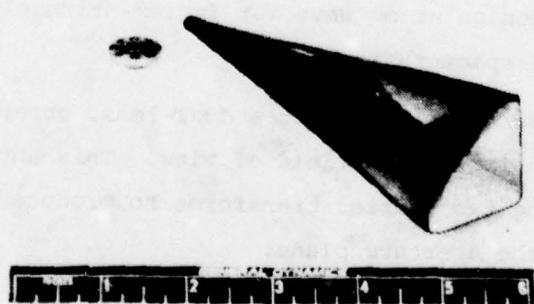
Figure 5-22. Graphite W-band Feed Horn

SIZE: 13.3" DIA X 33" DEEP
WEIGHT: 15.8 LB
BEAMWIDTH: 1.61°
NUMBER OF BEAMS: 121
SIDELOBE LEVEL: 18 DB
GAIN AT BEAM PEAK: 36.2 DB
GAIN AT MINIMUM: 31.0 DB

VARIABLE POWER DIVIDER
FEED NETWORK
FEED ARRAY

DIELECTRIC
APERTURE LENS

NUMBER OF BEAMS
GAIN
WEIGHT

BEAMWIDTH (DEGREES)
GAIN (dB)
WEIGHT (LB)
NUMBER OF BEAMS
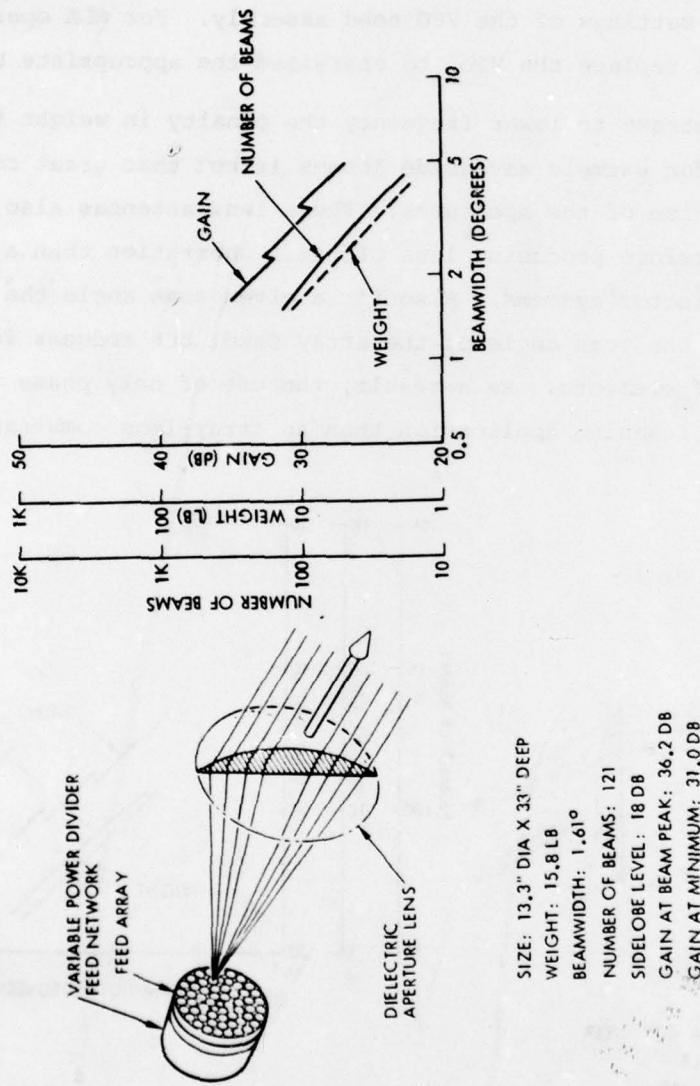
Figure 5-23. Dual Lens Array Antenna and Q-Band Phase Shifter

Other application of lens antennas is for MBA's as shown in Figure 5-24 and consisting of an aperture dielectric lens, a horn feed array and a variable power divided (VPD) network. For scanning beam operation, the antenna operates by routing the available power at the input port to the appropriate feed horns as selected by the phase settings of the VPD feed assembly. For MBA operation, a switching network will replace the VPD, to energized the appropriate beam.

At mm waves in contrast to lower frequency the penalty in weight for using dielectric lenses vs for example waveguide lenses is not that great considering the smaller physical size of the apertures. These lens antennas also are a symmetric system, therefore producing less off axis aberration than a lens/ reflector or dual reflector systems. Also for a given scan angle the magnification of the lens increases the scan angle of the array feed, but reduces its aperture area and the number of elements. As a result, the use of only phase arrays are less attractive for a scanning application than an array-lens combination.

SIZE: 13.3" DIA X 33" DEEP
WEIGHT: 15.8 LB
BEAMWIDTH: 1.61°
NUMBER OF BEAMS: 21
SIDELOBE LEVEL: 18 DB
GAIN AT BEAM PEAK: 36.2 DB
GAIN AT MINIMUM: 31.0 DB
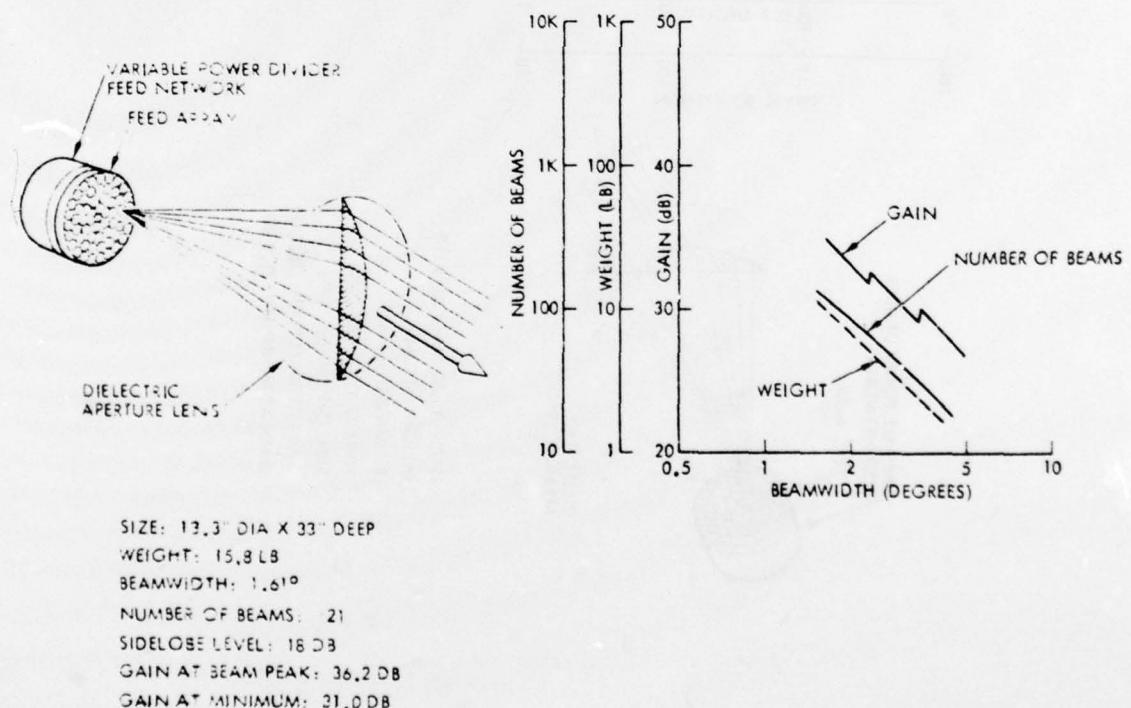
Figure 5-24. Multiple Beam Dielectric Lens